

Polar vortices in planetary atmospheres

Dann M Mitchell¹, Richard K Scott², William J M Seviour³, Stephen Thomson⁴, Darryn W. Waugh⁵, Nicholas A Teanby⁴, and Emily R Ball¹

¹Cabot Institute for the Environment

²University of St Andrews

³University of Exeter

⁴University of Bristol

⁵Johns Hopkins University

November 22, 2022

Abstract

Among the great diversity of atmospheric circulation patterns observed throughout the solar system, polar vortices stand out as a nearly ubiquitous planetary-scale phenomenon. In recent years there have been significant advances in the observation of planetary polar vortices, culminating in the fascinating discovery of Jupiter’s polar vortex clusters during the Juno mission. Alongside these observational advances has been a major effort to understand polar vortex dynamics using theory, idealised and comprehensive numerical models, and laboratory experiments. Here we review our current knowledge of planetary polar vortices, highlighting both the diversity of their structures, as well as fundamental dynamical similarities. We propose a new convention of vortex classification, which adequately captures all those observed in our solar system, and demonstrates the key role of polar vortices in the global circulation, transport, and climate of all planets. We discuss where knowledge gaps remain, and the observational, experimental, and theoretical advances needed to address them. In particular, as the diversity of both solar system and exoplanetary data increases exponentially, there is now a unique opportunity to unify our understanding of polar vortices under a single dynamical framework.

Polar vortices in planetary atmospheres

Dann M. Mitchell^{1,2}, Richard K. Scott³, William J. M. Seviour^{4,5}, Stephen I. Thomson⁴, Darryn W. Waugh⁶, Nicholas A. Teanby⁷, Emily R. Ball^{1,2}

¹Cabot Institute for the Environment, University of Bristol, Bristol, BS8 1SS, UK

²School of Geographical Sciences, University of Bristol, Bristol, BS8 1SS, UK

³School of Mathematics and Statistics, University of St Andrews, St Andrews, United Kingdom, UK

⁴Department of Mathematics, University of Exeter, Exeter, UK

⁵Global Systems Institute, University of Exeter, Exeter, UK

⁶Department of Earth and Planetary Sciences, The Johns Hopkins University, Baltimore, Maryland, USA

⁷School of Earth Sciences, University of Bristol, Wills Memorial Building, Queens Road, Bristol, BS8

1RJ, UK

Polar vortex, planet, exoplanet, dynamics, atmosphere

Key Points:

- Earth is not unique in having polar vortices, every well-observed planetary body with a substantial atmosphere appears to have at least one in each hemisphere.
- The range of planetary polar vortices in our solar system is extremely diverse, but much of their character can be explained in terms of the fluid dynamics developed for Earth.
- A novel classification of polar vortices into those with predominantly circumpolar flow (Type I) and those with large zonal asymmetries (Type II) encapsulates all polar vortex types that we know about.

Corresponding author: Dann Mitchell, d.m.mitchell@bristol.ac.uk

22
23
24
25
26
27
28
29
30
31
32
33
34
35
36
37

Abstract

Among the great diversity of atmospheric circulation patterns observed throughout the solar system, polar vortices stand out as a nearly ubiquitous planetary-scale phenomenon. In recent years there have been significant advances in the observation of planetary polar vortices, culminating in the fascinating discovery of Jupiter’s polar vortex clusters during the Juno mission. Alongside these observational advances has been a major effort to understand polar vortex dynamics using theory, idealised and comprehensive numerical models, and laboratory experiments. Here we review our current knowledge of planetary polar vortices, highlighting both the diversity of their structures, as well as fundamental dynamical similarities. We propose a new convention of vortex classification, which adequately captures all those observed in our solar system, and demonstrates the key role of polar vortices in the global circulation, transport, and climate of all planets. We discuss where knowledge gaps remain, and the observational, experimental, and theoretical advances needed to address them. In particular, as the diversity of both solar system and exoplanetary data increases exponentially, there is now a unique opportunity to unify our understanding of polar vortices under a single dynamical framework.

38

Plain Language Summary

39
40
41
42
43
44
45
46
47
48
49
50

Polar vortices are often described as the rotational motion of air in the polar regions of planets, this includes large vortices where flow circumnavigates the pole and smaller vortices that are centered within polar regions. The most commonly discussed polar vortices are those in Earth’s stratosphere, which have given rise to the ozone hole. More recently a number of other circulation patterns have been described as polar vortices, on Earth, and other planets. We review key features of these different polar vortices, and explain their similarities and differences using decades of theory, observations and modelling from the geophysical fluid dynamics community. We review how the different dynamical and chemical structures evolve as features of the polar vortex structures, and why they are integral to the makeup of planetary atmospheres. We conclude by summarising the latest knowledge on potential polar vortices outside of our solar system, which to date are only theorised.

51

52

1 Introduction

53
54
55
56
57
58
59
60
61
62

A nearly ubiquitous feature of planetary atmospheres in the solar system are rapidly rotating flows in polar regions, that are generally referred to as polar vortices. These features may be explained by consideration of basic physical constraints. At the most fundamental level, rapidly rotating planets have a minimum of angular momentum on the axis of rotation, and a maximum at the equator. Due to their rotation, planetary bodies may be expected to develop polar cyclonic flow as a result of transport of air between different latitudes, which will tend to increase the angular momentum at high latitudes, and decrease it at low latitudes. Such transport may arise through a variety of forms, including turbulence and wave stresses or the induced circulation arising from local heating or cooling anomalies (Andrews et al., 1987).

63
64
65
66
67
68

Transport of angular momentum alone, however, cannot be used directly to determine the development of cyclonic polar motions because background rotation and density stratification combine to place further dynamical constraints on the nature of the transport. An elegant way to view these constraints is through another dynamical quantity, the potential vorticity (PV), closely related to angular momentum and its conservation. PV, q , may be defined as

$$q = \frac{\zeta_a \cdot \nabla\theta}{\rho}, \quad (1)$$

69

70 where ζ_a is the absolute vorticity vector, $\nabla\theta$ is the potential temperature gradi-
 71 ent, and ρ is the air density. The material conservation of PV on fluid particles is essen-
 72 tially a statement of local angular momentum conservation. In contrast to angular mo-
 73 mentum, an atmosphere at rest has maximum PV over the pole, equal to the product
 74 of the planetary rotation rate and background density stratification (Equation 1). We
 75 refer to this resting maximum as the polar planetary PV. Material conservation of PV
 76 then implies that, again in the absence of other forces, transport alone cannot cause lo-
 77 cal PV values to increase beyond the polar planetary value. This property contains im-
 78 plicitly the dynamical constraints governing angular momentum transport in the pres-
 79 ence of density stratification, at least for geostrophic flows. One consequence, for exam-
 80 ple, is that Rossby wave breaking, one of the dominant dynamical processes responsi-
 81 ble for changes to the zonally symmetric atmosphere, may not on its own cause an in-
 82 crease in angular momentum (Wood & McIntyre, 2010).

83 To illustrate, in Earth’s stratosphere the winter polar vortex is ultimately a result
 84 of local diabatic cooling in the polar night. Although such thermal forcing does not ap-
 85 pear directly as a forcing of angular momentum, the induced circulation alters angular
 86 momentum through poleward transport, while the associated changes to the stratifica-
 87 tion lead to an associated PV increase, resulting in values significantly in excess of the
 88 polar planetary value (Andrews et al., 1987). Another way of understanding the increase
 89 in PV in terms of angular momentum transport is through the impermeability theorem,
 90 which states that the total PV between isentropic surfaces (surfaces of constant poten-
 91 tial temperature) must be conserved, even in the presence of diabatic forcing (Haynes
 92 & McIntyre, 1990). Cooling thus leads to an increase in concentration of PV through
 93 tightening of the isentropes.

94 The above considerations suggest that polar vortices will always be cyclonic and
 95 dependent ultimately on the planets rate of rotation (Table 1 lists some useful planetary
 96 parameters, for comparison). Beyond that, however, there is no well-established defini-
 97 tion for the term *polar vortex*. A polar vortex has become synonymous with multiple at-
 98 mospheric features, often meaning a different thing to different communities, even for
 99 a single planet. For instance, on Earth the term polar vortex has been used to refer to
 100 three distinct atmospheric features: a stratospheric polar vortex and a tropospheric po-
 101 lar vortex that have strong winds that encircle the pole, as well as smaller scale tropopause
 102 polar vortices that lie in polar region (Vaughn et al., 2017). Polar vortex has also been
 103 used in reference to different features on Venus (Sánchez-Lavega et al., 2017) and Sat-
 104 urn (Fletcher et al., 2018). These vortices have different structures, genesis, and main-
 105 tenance mechanisms, but a commonality is that they correspond to coherent regions of
 106 potential vorticity. While the potential vorticity dynamics discussed above are near-universal,
 107 there are also many significant differences between the structures of planetary polar cir-
 108 culations, which motivates us to further refine the definition into two types, such that
 109 we employ the following definition:

	a (10 ³ km)	Day (Earth = 1)	Obliquity (deg)	R _o	L _d / a
Venus	6.05	117	177	10	70
Earth	6.37	1	23.45	0.1	0.3
Mars	3.40	1.03	23.98	0.1	0.6
Jupiter	71.4	0.41	3.13	0.02	0.03
Saturn	60.3	0.44	26.73	0.06	0.03
Uranus	25.6	0.72	97.77	0.1	0.1
Neptune	24.8	0.67	28.32	0.1	0.1
Titan	2.58	16	27	2	10

Table 1. Planetary parameters relevant for the discussion of polar vortices. The day values are normalised to Earth. The second from last column shows the Rossby number estimated at mid-latitudes. The final column shows an estimate of the ratio of the Rossby Deformation Radius, L_d , to the planetary radius, a , evaluated at mid-latitudes. The obliquity values were taken from F. W. Taylor (2010) and all other values were taken from Showman et al. (2010), and readers are referred there for the full calculation and assumptions.

A polar vortex is a coherent structure with absolute potential vorticity that is larger than the polar planetary potential vorticity, and that is centered over or near the pole. This can be split into two types:

- **Type I: flows in which there is a predominantly circumpolar cyclonic flow. Examples include the winter polar circulations of Earth and Titan’s stratosphere and Mars’ lower atmosphere.**
- **Type II: flows of smaller horizontal scale in which zonal asymmetries are large enough that strong circumpolar flow is absent or of secondary importance. Examples include the Jovian vortex clusters, or synoptic-scale tropospheric polar cyclones on Earth.**

110

This classification is not the only possible one and even within each vortex Type, there exists a great diversity in vortex circulation patterns. On Earth, Mars and Saturn’s moon, Titan, there is a single near-circular Type I vortex, with strong circumpolar winds, at the winter pole, but the detailed structure and variability differs between the vortices (D. M. Mitchell et al., 2015; Teanby et al., 2008). In general, single polar vortices also exist in each hemisphere on Saturn and Venus, but with more varied shapes: A summer-time hexagonal wave surrounds that in Saturn’s northern pole (Fletcher et al., 2018), while the polar vortex core on Venus has a highly variable shape, with significant morphological changes on timescales of days (Garate-Lopez et al., 2013). In contrast to the other planets, there is not a single vortex at the poles of Jupiter but rather multiple rapidly rotating structures, with differing numbers and configuration between hemispheres (Adriani et al., 2018).

The cause of many of the differences in planetary polar vortices are not known, and there is a need for a better understanding of the fundamental processes controlling the formation, structure, and evolution of polar vortices. This is needed not only to understand the atmospheric circulation on each planet, but also to understand the atmospheric trace species chemistry. Unique transport, microphysical, and chemical processes can occur within polar vortices that result in significant differences in the composition within and outside the vortices. Perhaps, the most well-known is the ozone depletion and formation of the Antarctic ozone that occurs within Earth’s stratospheric polar vortices (Farman et al., 1985). In addition, condensation (and seasonal removal of) CO_2 occurs within the

111

112

113

114

115

116

117

118

119

120

121

122

123

124

125

126

127

128

129

130

131

132 Martian polar vortices (Haberle et al., 2017), and there are enhanced concentrations of
 133 complex hydrocarbons and formation of ice clouds in Titan’s polar vortices (Teanby et
 134 al., 2017; de Kok et al., 2014; Vinatier et al., 2018). Thus, understanding polar vortex
 135 dynamics and transport is key for understanding Earth’s ozone hole, the condensation
 136 of carbon dioxide at Mars’ polar ice caps, the chemistry of Titan’s polar regions, and most
 137 likely microphysical-chemical processes occurring in the polar regions of other planets
 138 and exoplanets.

139 Here we review our current knowledge of the structure and dynamics of planetary
 140 polar vortices. In Section 2 we discuss our knowledge of Earth’s polar vortices as the best
 141 observed ‘archetype’ of a polar vortex. In Section 3 we highlight what observations tell
 142 us about the diversity of polar vortices on other planets. In Section 4 we discuss devel-
 143 opments in theory and idealized- through to comprehensive- numerical models which have
 144 helped to explain many of the observed features, with Section 5 also doing this for labo-
 145 ratory experiments. Throughout, we highlight both the diversity, as well as fundamen-
 146 tal dynamical similarities between vortices on different planets. We discuss where knowl-
 147 edge gaps remain, the observational, experimental, and theoretical advances needed to
 148 address them, and, in Section 6, the possible range of vortices that may exist on the plan-
 149 ets in other solar systems.

150 **2 An archetype: Earth’s stratospheric polar vortices**

151 Earth’s Type I stratospheric polar vortex is not visible to the naked eye because
 152 there are no vortex-scale cloud structures associated with it. However, the vortex has
 153 been observed using meteorological fields from multiple measuring systems; initially from
 154 stratosphere-penetrating radiosondes and rocketsondes (Gutenberg, 1949; Scherhag, 1952),
 155 but more recently from satellite measurements (Wright et al., 2021). The vortices can
 156 also be seen in satellite measurements of trace gases. Most notably, measurements of the
 157 Antarctic ozone hole that forms inside the Southern Hemisphere vortex (Schoeberl & Hart-
 158 mann, 1991).

159 The stratospheric polar vortices are most readily characterised by strong circum-
 160 polar westerlies which maximize at around 60° latitude, from just above the tropopause
 161 (~ 150 hPa) into the mesosphere (above 1 hPa; see Figure 1). These strong westerlies form
 162 in autumn when there is no solar heating in polar regions, strengthen during winter as
 163 a consequence of the large-scale temperature gradients, and then weaken and become
 164 weak easterlies in spring-summer as sunlight returns to the polar regions e.g., (Waugh
 165 & Polvani, 2010).

166 Historically, Earth’s vortices were analyzed in terms of zonal winds or geopoten-
 167 tial height but more dynamical insight can be gained by using potential vorticity (Hoskins
 168 et al., 1985; Andrews et al., 1987). Earth’s stratosphere is highly stably stratified and
 169 mostly stable to both barotropic and baroclinic disturbances as PV generally increases
 170 in magnitude monotonically towards the pole. The polar vortices in both hemispheres
 171 have strong gradients in PV marking the vortex edge which acts as a mixing barrier be-
 172 tween the vortex interior and the lower latitude surf zone (Figure 1b).

173 In the Northern Hemisphere the stable vortex state (Figure 2, left) can be disrupted
 174 by upward propagating Rossby and gravity waves. The planetary waves are generally
 175 filtered to low wavenumbers around the tropopause because higher wavenumber waves
 176 cannot propagate through the strong stratospheric westerly winds (Charney & Drazin,
 177 1961), leading to mainly wavenumber 1 and 2 disturbances on the polar vortex (Figure
 178 2 middle and right). These events are extreme, often causing localised heating of $>70^\circ\text{C}$
 179 over a couple of days, and in many cases resulting in the complete breakdown of the po-
 180 lar vortex, either by displacing the polar vortex far from the pole, or splitting the par-
 181 ent vortex into two child vortices (Charlton & Polvani, 2007). Such events are termed

182 Sudden Stratospheric Warmings (Baldwin et al., 2020) and often result in tropospheric
 183 jet disturbances and associated extreme cold weather over Europe and North America
 184 (Baldwin & Dunkerton, 2001; Kolstad et al., 2010; D. M. Mitchell et al., 2013; Domeisen
 185 & Butler, 2020). However, while the causal relationship between the polar vortex break-
 186 down and surface weather is well documented, the exact linking-mechanisms are still de-
 187 bated (Kidston et al., 2015).

188 The upward propagating waves arise, in part, due to surface orography and land-
 189 ocean contrast which are more abundant in the Northern Hemisphere. A consequence
 190 of this is that there are fewer and weaker waves in the Southern Hemisphere and the po-
 191 lar vortex is stronger and more stable than its northern counterpart. The seasonal life-
 192 time of the southern vortex is longer, and there has only been one major southern Sud-
 193 den Stratospheric Warming in the 60 years of observations, as opposed to ~ 45 reported
 194 cases in the northern hemisphere (Krüger et al., 2005; Charlton & Polvani, 2007; But-
 195 ler et al., 2017).

196 One consequence of the strengthened southern vortex is that the vortex edge is a
 197 strong mixing barrier, isolating polar air which allows it to get extremely cold. This re-
 198 sults in the formation of polar stratospheric clouds throughout the vortex every winter,
 199 providing sites for heterogeneous reactions and leading to chemical destruction of ozone
 200 and formation of the Antarctic ozone hole within the vortex (Schoeberl & Hartmann,
 201 1991). The weaker northern vortex does not get so cold, and the formation of polar strato-
 202 spheric clouds and depletion of ozone is less in the northern polar vortex (Ivy et al., 2017).

203 The influence of Earth’s polar vortex is not limited to the stratosphere, and vari-
 204 ability in the vortex has an impact on surface weather and climate. This includes trends
 205 in Southern Hemisphere summer circulation, and associated weather, and ocean circula-
 206 tion, which have been linked to the ozone hole induced strengthening of the Antarc-
 207 tic polar vortex (Thompson et al., 2011).

208 Given the importance of the polar vortices on Earth, it is perhaps unsurprising how
 209 much research has focussed on them. These theoretical, modeling and laboratory stud-
 210 ies are reviewed in Section 4, along with the links to other planetary bodies.

211 **3 The diversity of polar vortices**

212 **3.1 Terrestrial planets in the solar system**

213 **3.1.1 Venus**

214 Mercury does not have a substantial atmosphere, so the closest planet to the Sun
 215 with polar vortices is Venus (Taylor et al., 1979). Data on the polar vortices from Venus
 216 were first collected in 1974 by Mariner 10, with a number of additional flyby and orbiter
 217 missions ever since, culminating in the Akatsuki craft making orbit in December 2015
 218 and remaining operational ever since. While space-based missions to Venus’ atmosphere
 219 have been numerous, with the atmosphere having been imaged earlier than any planet
 220 other than Earth, the longevity and sophistication of the missions have not necessarily
 221 been on par with some missions sent to Mars, Jupiter, Saturn and Titan, at least when
 222 considering the polar atmospheres.

223 The atmosphere of Venus is thick, with numerous cloud layers and strong super-
 224 rotation (Read & Lebonnois, 2018). The Venusian atmospheric circulation has been re-
 225 viewed in detail by Sánchez-Lavega et al. (2017), including a dedicated section on the
 226 polar vortices and cold collars. As noted in Sánchez-Lavega et al. (2017), the term po-
 227 lar vortex has been used to describe different polar features on Venus, namely a coher-
 228 ent hemispheric-scale swirling wind pattern (Figure 3), and a highly energetic tropical-
 229 cyclone-like vortex that precesses around the pole, and is surrounded by a region of colder

230 air “the cold collar” (Figure 4). Here, we refer to the former as “the polar vortex”, and
 231 the latter as “the polar vortex eye”. Due to the small axial tilt of Venus (Table 1), there
 232 are no strong seasonal influences, so polar vortex structures exist all year round and share
 233 many similarities between hemispheres such as depressed cloud layers inside the vortices
 234 which indicate downwelling. It was these cloud features that first pointed towards the
 235 presence of the southern polar vortex (V. Suomi, 1974; V. E. Suomi & Limaye, 1978),
 236 and later the northern one (F. W. Taylor, 2014).

237 At the cloud top level the southern polar vortex extends to mid-latitudes and is
 238 elliptical, which might be indicative of wave 2 planetary wave forcing (V. E. Suomi &
 239 Limaye, 1978) (Figure 3). Understanding the exact latitudinal extent of the polar vor-
 240 tices has proven difficult, especially given the variable vortex morphology (e.g. Figure
 241 4). This difficulty has arisen, in part, due to the lack of in situ wind measurements (Gierasch
 242 et al., 1997), although approximations have been derived, e.g. through using thermal sound-
 243 ing measurements (Piccialli et al., 2012), tracking of cloud features (Limaye & Suomi,
 244 1981), or through a full Venusian reanalysis (which are a combination of observations
 245 and atmospheric modelling to provide a holistic estimate of the climate; (Sugimoto et
 246 al., 2019)). By considering a derived zonal mean PV quantity, Piccialli et al. (2012) claimed
 247 that there was no latitude of significantly increased PV gradient at most altitudes, which
 248 would have indicated a presence of a vortex mixing barrier (i.e. a vortex edge). Their
 249 analysis was based on cyclostrophically balanced flow inferred from limited latitudinal
 250 thermal gradients, so this could have led to artificially damped PV gradients. In one re-
 251 gion of the atmosphere, around the top of the cloud layer (~ 58 km), they did show some
 252 increase in the strength of the latitudinal PV gradient, and this would coincide with co-
 253 herent PV structures derived from Venus Express (Garate-Lopez et al., 2016) (see also
 254 Figure 4). In both Piccialli et al. (2012) and Limaye et al. (2009) this maximum seems
 255 to be at $\sim 65^\circ\text{S}$ in the southern hemisphere, although an equivalent has not been esti-
 256 mated for the northern hemisphere. Limaye et al. (2009) indicate that at this altitude,
 257 the vortex may be annular, although this is not observed by Piccialli et al. (2012) or in
 258 zonal mean PV analyses (Figure 1a).

259 Within this larger vortex structure, the most striking feature is the central core,
 260 which due to its chaotic nature sometimes appears as a dipolar ‘S’ shape, a monopole,
 261 or a tripole and is indicated by the bright UV regions in Figure 4. It is present in both
 262 hemispheres, but based on current data is particularly apparent in the Southern Hemi-
 263 sphere (Figure 4) where it rotates at a much faster rate than its northern counterpart
 264 (Piccioni et al., 2007). Analogous features are seen in Earth’s tropical cyclones leading
 265 to speculation that some of the controlling factors between the two are the same, although
 266 the spatial scale and lifetimes of the two are very different (Limaye et al., 2009). For in-
 267 stance, while Venus’ wider polar vortex structures have persisted throughout observa-
 268 tions thereby existing for at least 40 years (and probably much longer), the more vari-
 269 able features in the core are generated through dynamical instabilities, lasting a couple
 270 of days, which is longer than similar features in Earth’s tropical cyclones. The three or-
 271 bits shown in Figure 4 reveal three very different southern vortex eye structures, but are
 272 just a small subset on Venusian morphology’s that have been observed (Garate-Lopez
 273 et al., 2016).

274 The brighter cloud-free regions observed on Venus may indicate downwelling (Garate-
 275 Lopez et al., 2016) from the poleward and descending branches of the Hadley circula-
 276 tion (Luz et al., 2011), although there is still some debate in the literature over this ow-
 277 ing to the lack of meridional wind measurements poleward of 70° (Sánchez-Lavega et al.,
 278 2017). It has been proposed that the vortices formed due to a combination of diurnal
 279 tides, and baroclinic waves (Yamamoto & Takahashi, 2015). The complex structural fea-
 280 tures of the polar vortex eyes seem to be present at multiple vertical depths, but the vor-
 281 tices are highly baroclinic in nature (Garate-Lopez et al., 2013, 2015, 2016).

282

3.1.2 Mars

283

284

285

286

287

288

289

290

291

292

293

Mars' polar atmosphere has received more focused observations than Venus. So much so that we even have multiple reanalysis data sets (Montabone, Marsh, et al., 2014; Greybush et al., 2012; Holmes et al., 2020). Reanalysis data show that the Martian polar vortices, which extend throughout the troposphere (~ 0 -50 km), decrease in area with height and retain the same orientation in the vertical (D. M. Mitchell et al., 2015) (Figure 1c). A striking annular PV structure is clear in observations, reanalysis and some models, with the vortex edge coinciding with the edge of the meridional circulation (Banfield et al., 2004; D. M. Mitchell et al., 2015). Zonal averages of potential vorticity show a maximum at around 75 - 80° , with opposing PV gradients on either side of this maximum. This implies unstable flow (Andrews, 1987) and suggests there must be a stabilising force acting on the polar circulation.

294

295

296

297

298

299

300

301

The ring of PV is thought to form because of the latent heating due to CO_2 condensation inside the vortex, which decreases PV there (Toigo et al., 2017). The PV field is relatively smooth when averaged over >30 Martian days, but on shorter timescales much smaller scale PV features are apparent (Waugh et al., 2016). There is some suggestion that these features are associated with spatially inhomogeneous latent heat released during the CO_2 transition from gaseous to solid form, with atmospheric aerosol acting as cloud condensation nuclei (Rostami et al., 2018), but they may also be due to instabilities (Seviour et al., 2017), or simply artifacts of the reanalysis.

302

303

304

305

306

307

308

309

310

311

312

313

314

315

316

317

318

319

In most years the characteristics (e.g. size and shape) of the Martian vortex are relatively constant throughout the winter, but during years with hemispheric-scale dust storms there can be a major disruption through shifting the descending branch of the overturning circulation (Wang, 2007; Guzewich et al., 2016; Ball et al., 2021). Due to the change in dynamics and radiative absorption, “rapid polar warming” events can occur on daily timescales (D. M. Mitchell et al., 2015). A global dust storm in Martian year 28 had a particularly striking impact on the northern vortex, as seen in Figure 5a. The major growth of this dust storm likely occurred in the southern mid-latitudes, shortly before the northern winter solstice (Wang & Richardson, 2015). Zonal winds were weakened by up to 40 ms^{-1} compared to a multiannual average of later years in which no global dust storm occurred (Figure 5b). Potential vorticity in the vortex was also weakened significantly, with the annulus of high PV being completely destroyed (Ball et al., 2021). Regional dust storms, which do not encircle the planet but still have high dust loading over a large area ($> 1.6 \times 10^6 \text{ km}^2$) and last for multiple sols (Cantor et al., 2001), may also influence polar vortex dynamics. Large regional dust storms in the southern hemisphere have been shown to affect the northern vortex, such as the dust storm in Martian year 26 which caused the northern vortex to shrink and weaken in PV terms (Montabone, Mitchell, et al., 2014; D. M. Mitchell et al., 2015).

320

3.1.3 Titan

321

322

323

324

325

326

327

328

329

330

331

Mars is not the only Solar System example of an annular polar vortex. Saturn's largest moon, Titan, also has one, with stratospheric PV peaking at around 65° latitude (Teanby et al., 2008; Achterberg et al., 2011; Sharkey et al., 2020b) (Figures 1d and 6). Since Titan orbits in Saturn's equatorial plane it shares the same seasonal variations, completing a full Titan year in ~ 29.5 Earth years. Titan is tidally locked, with one hemisphere always facing Saturn, so has a day length of 15.9 Earth days, equal to its orbital period around Saturn. However, like Venus, Titan's atmosphere experiences super-rotation (Read & Lebonnois, 2018). Radiative timescales in Titan's polar stratosphere are $\sim 10^7$ s at 0.1 hPa, much shorter than Titan's year, allowing the vortices to respond rapidly to seasonal forcing such that they peak in strength in the winter hemisphere (Achterberg et al., 2008, 2011; Teanby et al., 2019; Vinatier et al., 2020). Due to the large Rossby

332 deformation radius on Titan (Table 1), the vortices are large yet still respond to pertur-
 333 bations as a coherent structure.

334 Some of the most valuable observations for understanding Titan’s polar vortices
 335 are from the Cassini mission, which covers just under half a Titan year from northern
 336 mid-winter to northern summer solstice. Cassini’s high orbital inclination phases allowed
 337 Titan’s winter polar regions to be observed in detail, which is not possible from Earth-
 338 based observatories because Titan’s winter pole faces away from the Earth (Table 1). Cassini’s
 339 Composite InfraRed Spectrometer (CIRS) (F. M. Flasar et al., 2004; Nixon et al., 2019)
 340 is particularly valuable as it allows detailed measurements of temperature and trace gases
 341 directly over both poles (Achterberg et al., 2011; Teanby et al., 2019; Coustenis et al.,
 342 2020; Sharkey et al., 2020b; Sylvestre et al., 2020; Vinatier et al., 2020) (Figure 6).

343 Cassini observations revealed a rapid transition in the southern polar circulation
 344 direction just after northern spring equinox (Teanby et al., 2012) and the subsequent early
 345 formation stages of the south polar vortex (Teanby et al., 2017). Conversely the north-
 346 ern vortex was observed while fully formed and during its decline as the seasons changed
 347 from northern winter to northern summer. Modelling (Lebonnois et al., 2012) and ex-
 348 trapolations of the available observations (Teanby et al., 2019) suggest northern and south-
 349 ern vortices are similar in nature, but this has yet to be observationally verified.

350 The latitudinal extent of the vortices are greater on Titan than Earth and Mars
 351 (F. Flasar & Achterberg, 2008) and are almost perfectly zonally-symmetric (Sharkey et
 352 al., 2020a). Observations of trace gases in Titan’s polar regions can be used to indirectly
 353 probe the circulation. Many of these gases are photochemically produced at high alti-
 354 tudes (i.e. above the stratosphere) and are removed by condensation in the lower strato-
 355 sphere. This source-sink relationship sets up vertical gradient profiles that have increas-
 356 ing relative abundance with increasing altitude, with short lifetime species having stronger
 357 gradients (Teanby et al., 2009). Subsidence caused by the global overturning circulation
 358 advects enriched air down to stratospheric altitudes, causing strong enhancements in abun-
 359 dances that can be used to probe the atmospheric dynamics. Observations show that
 360 strong PV gradients of the vortex edge effectively isolate short-lived tracer enriched air
 361 (Sharkey et al., 2020b). For example, Figure 6c shows that HC_3N , which has a lifetime
 362 much less than a Titan year, is confined within the vortex. However, for longer lived species
 363 there is evidence that tongues of gas extend away from the polar vortex suggesting a role
 364 for secondary circulations or wave dynamics and instabilities in cross-boundary mixing
 365 (Teanby et al., 2008; Vinatier et al., 2020).

366 The polar trace gases on Titan may also play a more active role in the circulation
 367 by significantly enhancing radiative cooling at the poles. Extreme enrichment of these
 368 photochemically produced gases has been suggested to affect the radiative balance over
 369 the poles, leading to unexpectedly cold stratospheric temperatures during early winter
 370 and a potential dynamical-radiative feedback (Teanby et al., 2017). The main coolers
 371 of this highly enriched polar mesosphere are C_3H_4 , C_4H_2 , and HC_3N (Teanby et al., 2017).
 372 These are dynamically enriched by factors of 10–1000 compared to equatorial regions,
 373 so significantly alter the radiative balance of the vortex, and may be enough to cause a
 374 sudden cooling. These extremely cold stratospheric temperatures were observed for the
 375 first time during south polar vortex formation by Cassini (Teanby et al., 2017) (Figure 6a).
 376 However, these extremely cold temperatures were not seen in the more evolved north-
 377 ern vortex, or indeed in the mid-winter southern vortex (Figure 6a), suggesting that subsidence-
 378 induced adiabatic heating is more important than radiative cooling once Titan’s vortex
 379 is fully formed (Teanby et al., 2017). This dynamic-radiative feedback is so far thought
 380 to be unique to Titan; on Earth (and indeed Mars and Venus) this is not the case, as
 381 CO_2 is the dominant radiative cooling agent, which is well mixed and so not redistributed
 382 and concentrated into subsiding polar regions in the same way (Teanby et al., 2017).

3.2 Gas giant planets in the solar system

Polar vortices are not unique to terrestrial planetary bodies; we have observed them on all four of the solar system giant planets (Figure 3). We have known about the polar vortices on Saturn, Uranus and Neptune for decades, because ground-based telescopes have been able to observe them during the relevant seasons. This is only possible because the obliquity of these planets is large, in all cases greater than 25° (see Table 1).

3.2.1 *Jupiter*

Jupiter, with an obliquity of $\sim 3^\circ$, however, has only very recently had its polar region observed during polar orbits of the Juno probe (Bolton et al., 2017). Other missions flying by the planet were confined to Jupiter’s equatorial plane, so suffered the same limitations as Earth-based measurements. The Juno spacecraft was able to view Jupiter’s polar regions for the first time, using both visible and infrared (IR) sensors, and revealed a fascinating and unexpected Type II vortex at both poles. Located $\sim 0.5^\circ$ offset from the North Pole, there exists a central, cyclonic vortex consisting of small-scale cloud structures (Figure 3). The central vortex is surrounded by eight cyclonic vortices of similar diameter (4000-4500 km) that are likely to have similar rotation rates around their axis of rotation, as the central vortex rotation does, ranging from ~ 26 -60 hours, depending on the vortex. However, given observational uncertainty, there may be some progressive motion (Adriani et al., 2018). The eight surrounding vortices form a quadrilateral structure with each side being composed of a line of 3 vortices which alternate between cloudier and clearer structures (Figure 3).

The southern polar vortex only contains five vortices surrounding a central vortex. The vortices are larger in diameter by ~ 1500 km than those of the Northern Hemisphere, but are more spaced out, with clear gaps between the vortices filled with meso-scale wave and jet structures (see, for instance Figure 1 in (Adriani et al., 2018)). The central southern vortex has clearer cloud banding than its Northern counterpart, and the core of the vortex is far more elliptical than any of the other vortices (Adriani et al., 2018). Unlike in the Northern Hemisphere, there is a clear counter-clockwise progressive motion of the five surrounding vortices relative to the central vortex’s rotation speed.

With only a single targeted mission to observe Jupiter’s atmosphere, it is hard to discern the vertical extent of the polar vortices, and as such it is not obvious which layers of the atmosphere these exist in, or whether the structure is barotropic or baroclinic in nature. As the observations are currently from visible and IR sensors, they are mainly looking at the cloud ‘tropospheric’ layer, although this does not preclude vortices at other levels in the atmosphere. With such a short observation period it is not clear how these vortex clusters will change with time, although the currently observed period suggests some migration of the vortices. The existence of stable Northern and Southern polar vortices at the same time is unusual for planets, although due to its axial tilt Jupiter does not really experience seasons and seasonality on other planets is often associated with the forming and breakdown of polar vortices, i.e. through changes in latitudinal temperature gradients.

3.2.2 *Saturn*

Unlike on Jupiter, the polar vortices in Saturn’s stratosphere (~ 200 -300 km above the cloud layer) are seasonal, but in the opposite sense to Earth, such that they are established before the summer and breakdown before winter (Orton & Yanamandra-Fisher, 2005; Fletcher et al., 2008). The Cassini probe has allowed us to observe Saturn’s polar circulation in unprecedented detail (Baines et al., 2009; Sayanagi et al., 2018). As with most other known planetary polar vortices, a single Type I vortex exists centred on each pole, but smaller (typically 1000-1500 km in diameter) cyclonic and anti-cyclonic

432 features are also observed (Antuñano et al., 2018), reminiscent of Type II vortices, and
 433 these can be seen as bright spots in Figure 3. Both of Saturn’s stratospheric polar vor-
 434 tices are circular in nature, with the polar vortex edge reaching speeds of 140-160 ms^{-1}
 435 (Antuñano et al., 2015; Sayanagi et al., 2017). The peak potential vorticity in both hemi-
 436 spheres is at the pole, with the southern polar vortex exhibiting higher absolute values
 437 (Antuñano et al., 2019).

438 A distinctive feature in the northern hemisphere is that the vortex is surrounded
 439 by a zonal wavenumber-6 ‘hexagonal’ westerly jet which peaks at around 100 ms^{-1} . This
 440 jet was observed by Voyager in 1980 (Godfrey, 1988), and has persisted ever since, most
 441 likely resulting in two strong PV gradients within the polar region that constitute the
 442 strong cyclone vortex, and a nearby jet (Figure 3) (Scott & Polvani, 2006; Fletcher et
 443 al., 2018; Antuñano et al., 2019). While there exists a jet at a similar latitude in the south-
 444 ern hemisphere, it is weaker (Sayanagi et al., 2018), and does not have the same wavenumber-
 445 6 pattern, despite having similar potential vorticity gradients (and as such potential for
 446 instabilities) (Antuñano et al., 2019).

447 The polar vortices exist for >100 km in the vertical, covering both the stratosphere
 448 and troposphere, but it is not currently known how far below the visible cloud layer they
 449 extend (Sayanagi et al., 2018). The tropospheric polar vortices share many similar char-
 450 acteristics of the stratospheric ones, but importantly are present all year round, still with
 451 similar strengths though (Dyudina et al., 2008). In the Northern Hemisphere, the tro-
 452 pospheric polar vortex again has a close-by hexagonal jet (Allison et al., 1990). The tro-
 453 pospheric vortex is highly convective, with an inner and outer eyewall of cloud extend-
 454 ing to the tropopause (Dyudina et al., 2008). As with the other gas planets, the vortices
 455 on Saturn are associated with a warm polar region (Orton & Yanamandra-Fisher, 2005;
 456 Dyudina et al., 2009). There is a suggestion that within these polar vortices subsidence
 457 takes place, as evidenced from increased optical thicknesses of the stratospheric hazes
 458 and the location of the base of the tropospheric haze (Sanz-Requena et al., 2018).

459 **3.2.3 Uranus and Neptune**

460 The polar regions on the icy giants Uranus and Neptune are less well studied be-
 461 cause there have been no high-inclination space missions equivalent to Juno or Cassini
 462 for these planets, with only the single Voyager 2 flybys in 1986 and 1989 respectively.
 463 The Voyager observations of the polar regions are augmented with ground-based tele-
 464 scopic observations, with advances in adaptive optics and radio interferometry afford-
 465 ing detailed if sometimes rather oblique polar views (de Pater et al., 2014). Using the
 466 available observations, the strongest evidence of polar vortices comes from identifying
 467 polar clouds. Such features are observed in Uranus’ southern polar region, with a sym-
 468 metric vortex centred slightly off the pole, rotating with a period of ~ 24 hours and ex-
 469 tending out to 84°S (Karkoschka, 2015). Uranus’ North polar region also clearly has cloud
 470 or haze features (de Pater et al., 2015; Sromovsky et al., 2012) but no corresponding vor-
 471 tex edge is observed (Figure 3), suggesting Uranian vortices may be a seasonal phenomenon
 472 like on most other planets (Sanders, 2017; Brueshaber et al., 2019).

473 Neptune’s north polar region has been particularly difficult to observe due to its
 474 axial tilt shadowing it from Earth for a number of decades (Table 1), meaning the cir-
 475 culation features cannot be tracked (Karkoschka, 2015). However, in the Southern Hemi-
 476 sphere, a bright polar cloud structure has been observed which resembles the convective
 477 polar vortices on Saturn (Fletcher et al., 2015, 2012), and which has persisted since the
 478 Voyager era, far longer than other convective systems at lower latitudes on Neptune (Luszcz-
 479 Cook et al., 2010; Irwin et al., 2016). It has been reported that this region constituted
 480 a hot pole, and argued that it was due to seasonal heating (Orton et al., 2007), although
 481 it could also be a hole in the clouds, allowing for detection of warmer regions of the at-
 482 mosphere. As with Jupiter and Saturn, it is likely that this is a stable polar vortex, but

483 unlike those planets, the polar vortex on Neptune is significantly larger in latitudinal ex-
 484 tent, with the edge located at $\sim 80^\circ\text{S}$ (Luszcz-Cook et al., 2010).

485 **4 Theory and modelling**

486 Observations can only take us so far in our understanding of planetary polar vor-
 487 tices, in part because there are many aspects of a planetary system we cannot directly
 488 observe but also because it is not possible to test the controlling factors of the system
 489 by switching on or off certain processes or ‘forcings’. It is therefore necessary to com-
 490 bine observations with theory and a hierarchy of models to develop a fuller understand-
 491 ing of the polar vortices (Figure 7). In this section we give an overview of a range of com-
 492 plexity of models that can be used to understand polar vortices in some way. These range
 493 from very idealised models used to understand the basics of vortex dynamics, through
 494 to comprehensive models of individual planetary polar vortices.

495 Perhaps the simplest representation of a polar vortex is as a region of uniform po-
 496 tential vorticity, or ‘vortex patch’. Studies date back to Kirchhoff (Kirchhoff, 1876), with
 497 the original vortex stability results (Love, 1893) and sheared vortex regimes (Kida, 1981)
 498 still just as relevant today in understanding the stability of monopolar PV distributions,
 499 such as Earth’s stratospheric polar vortex (Matthewman & Esler, 2011). Elliptical per-
 500 turbations to the vortex edge may be readily generalized to any azimuthal wavenumber:
 501 the vortex patch again provides a convenient model for the study of finite amplitude Rossby
 502 waves on the edges of monopolar vortices and the dynamics of wave breaking (Dritschel,
 503 1986; Waugh & Dritschel, 1991; Polvani & Plumb, 1992).

504 Another straightforward generalization of the vortex patch model, relevant to cases
 505 of non-monopolar polar vortices, is by considering an annular distribution of uniform po-
 506 tential vorticity in which the potential vorticity maximum is located at a finite radius
 507 from the pole. Such configurations tend to be dynamically unstable. The linear stabil-
 508 ity of the equivalent distribution in planar Cartesian geometry, comprising a uniform strip
 509 of vorticity, was described originally by (Rayleigh, 1880). The original analysis has been
 510 subsequently modified to include the effects of nonlinearity and spherical geometry (Dritschel
 511 & Polvani, 1992) (Fig 7a) as well as the effect of finite deformation radius (Waugh & Dritschel,
 512 1991).

513 In both monopolar patch and annulus cases, the extension from two to three di-
 514 mensions is straightforward, if computationally more expensive. To the extent that many
 515 of the dominant dynamical processes are layerwise two-dimensional, the two-dimensional
 516 models still provide a useful dynamical framework in which to test hypotheses in many
 517 cases of interest. The idealization of uniform potential vorticity inside and outside the
 518 patch or annulus can be easily generalized to continuous distributions. The annulus model
 519 was recently used to study the growth of disturbances in the context of the annular Mar-
 520 tian polar vortex, which can be viewed, for example, as resulting from a competition be-
 521 tween dynamical instability and the restoring effects of radiative forcing (Seviour et al.,
 522 2017; Rostami et al., 2018; Scott et al., 2020). Another application is to the hexagonal
 523 wave structure observed near Saturn’s pole. While the hexagon exists on a jet surround-
 524 ing the more compact polar vortex at its centre, rather than the polar vortex itself, its
 525 development may again be examined in terms of the basic two-dimensional potential vor-
 526 ticity distributions. The simplest description is that of a wave on the edge of a vortex
 527 patch, following Deem and Zabusky (1978); Polvani and Dritschel (1993), though per-
 528 haps a more realistical picture is given in terms of the instability of an annular struc-
 529 ture coupled to a central patch (Rostami et al., 2017).

530 In a similar way, the study of arrays of vortex patches or point vortices, and the
 531 motions of single patches on a background planetary vorticity gradient can provide in-
 532 sight into the polar vortices on the gas giants. Polar cyclones on Saturn, Uranus and Nep-

533 tune may all be expected to arise under very general conditions as a result of vortex beta-
 534 drift, whereby coherent cyclones induce circulation patterns that result in a net poleward
 535 drift of the cyclone (Lam & Dritschel, 2001; O’Neill et al., 2016). This is of course also
 536 true for terrestrial planets, although often in the troposphere friction prevents vortices
 537 from reaching the pole. For instance, analogous to tropical cyclone drift to mid-latitudes
 538 on Earth. For Saturn, the poleward drift and subsequent merging of cyclones was demon-
 539 strated to result in persistent polar accumulation of cyclonic vorticity under general con-
 540 ditions and with no external forcings (Dyudina et al., 2008, 2009; Baines et al., 2009).
 541 Cyclones will migrate to the pole if their initial strength exceeds the potential vortic-
 542 ity at the pole by about 12% (Scott, 2011), a constraint that effectively limits polar ac-
 543 cumulation to vortices originally relatively close to the pole. The speed of poleward mi-
 544 gration is slower at smaller planetary Rossby deformation radius, L_d , which already gives
 545 a key to different in planetary polar vortices (Table 1). A closely related parameter, the
 546 planetary Burger number $Br = (L_d/a)^2$, where a is the planetary radius, has also been
 547 shown to be a key parameter controlling polar vortex regimes (M. E. O’Neill et al., 2015).
 548 When varied in conjunction with an energy potential parameter (this energy could take
 549 the form of, e.g. latent heat), then vortices that share characteristics of those observed
 550 on other planets can be established. Notably if the energy parameter is too small then
 551 cyclones cannot reach the pole before their energy is radiated away in the form of Rossby
 552 waves.

553 An attempt at fitting Jupiter’s vortices into this dynamical framework was sub-
 554 sequently undertaken (Brueshaber et al., 2019) and two additionally controlling param-
 555 eters were found (albeit less important than the Burger number). These were the ini-
 556 tial cyclone strength, and the ratio of the number of initial cyclones versus initial anti-
 557 cyclones. These additional parameters were found to modify the transitions between dif-
 558 ferent giant planet polar dynamical regimes, namely ice-giants and Saturn, but also to
 559 some extent Jupiter, although the observed configuration (Adriani et al., 2018) was not
 560 fully reproduced. Insight into the multiple vortex configurations on Jupiter can also be
 561 drawn from existing stability criteria obtained for arrays of point vortices or patches. While
 562 the original observations of the Jovian vortex arrays generated a certain degree of ex-
 563 citement, theoretical studies of the stability of such configurations date back to (Thomson,
 564 1883), who showed that an array of up to five regularly spaced point vortices forms a sta-
 565 ble configuration. Since then numerous studies have extended Thomson’s result by con-
 566 sidering, for example, background shear or the addition of a central vortex, both of which
 567 have a stabilizing effect (Schechter et al., 1999; Fine et al., 1995). A recent example in
 568 which a stable ring of vortices surrounds a central one in a Boussinesq atmosphere is shown
 569 in Figure 7d (Reinaud & Dritschel, 2019), although from these examples it is unclear as
 570 to why these clusters may form on Jupiter, but not the other gas giants.

571 The natural tendency of migrating vortices to merge at the pole is clearly not hap-
 572 pening on Jupiter, and it is likely that each Jovian cyclonic vortex is ‘shielded’ by a band
 573 of anti-cyclonic air on the vortex edge, acting to repel the sibling vortices (Li et al., 2020).
 574 Figure 8 show a shallow water simulation of this process as an example of how it may
 575 happen on Jupiter. An intruding shielded vortex migrates from low latitudes and reaches
 576 the cluster at day 17, rotating around the Type II polar vortex cluster until it finds a
 577 way in at around day 58, ultimately forming a new stable configuration. This type of
 578 process could explain the different numbers of vortices at Jupiter’s two poles, as well as
 579 the recently observed vortex migration.

580 From the combined theory and modelling discussed above, a natural question then
 581 arises: what aspects of polar vortices can be understood in terms of the freely evolving,
 582 unforced dynamics alone, and what aspects are intrinsically related to dynamical or ther-
 583 modynamical forcings present in the system? A suitable system for addressing this is the
 584 single-layer shallow water model, or its quasi-geostrophic approximation, representing the
 585 quasi-horizontal dynamics between two isentropic surfaces. Such a model may capture

586 the most relevant motions in a shallow atmosphere when f/N is large (where f is the
 587 Coriolis parameter, and N the Brunt–Väisälä frequency), possibly with additional ex-
 588 plicit forcings to represent the effects of parts of the atmosphere outside the layer of in-
 589 terest; the use of such forcings thus allows some fully three-dimensional effects to be in-
 590 cluded. The shallow atmosphere model has a long history of applications to the Earth’s
 591 winter stratospheric polar vortex, where many ideas of mixing and transport, surf zone
 592 formation, gradient intensification and the formation of transport barriers, have all been
 593 convincingly illustrated and analyzed (Polvani et al., 1995; Jukes, 1989) and it also cap-
 594 tures some of the key features of certain vortex breakdown events (Rong & Waugh, 2004;
 595 Matthewman & Esler, 2011; Liu & Scott, 2015). In these cases, the appropriate forcings
 596 are a relaxation on the layer thickness, representing the effects of radiative cooling in the
 597 polar night, and a bottom wave perturbation, representing the combined effects of all
 598 upward planetary wave propagation from the troposphere.

599 Non-Earth polar vortices may be forced in much the same way, with appropriate
 600 choice of radiative equilibrium and wave forcing. This approach was adopted recently
 601 to examine the persistence and dynamical stability of the annular polar vortex on Mars
 602 (e.g. Figure 7b), considering under what conditions such a vortex may persist in an ap-
 603 proximately zonally symmetric state, or alternatively break up transiently into a more
 604 eddy dominated regime (Seviour et al., 2017; Rostami et al., 2018). Different regimes
 605 are found to be governed by the strength of the annular forcing, the radiative relaxation
 606 timescale, as well as details of topographic forcing. Mixing and transport are altered dra-
 607 matically according to the regime and so understanding persistence is key to understand-
 608 ing atmospheric composition on Mars, and more generally on atmospheres with similar
 609 annular structures. Titan’s polar vortex is a key example here, with radiatively active
 610 tracer isolation and subsidence inside the vortex being key to its development and evo-
 611 lution (Teanby et al., 2017).

612 While the radiative forcing used by Seviour et al. (2017) is a natural and conve-
 613 nient way of forcing the basic annular structure, an alternative is to represent the lat-
 614 itudinal transport of angular momentum by the Hadley cell outflow, which on Mars and
 615 Titan can extend to 60° (Figure 3) latitude or beyond in the northern hemisphere win-
 616 ters (Waugh et al., 2016; Teanby et al., 2019; Sharkey et al., 2020a). Again, while the
 617 Hadley cell itself is an intrinsically three-dimensional circulation, it may be represented
 618 in the shallow water model by an appropriate mass source/sink in the layer thickness
 619 (Shell & Held, 2004). This approach was adapted to the Mars regime by allowing a stronger
 620 and more asymmetric Hadley cell (Scott et al., 2020). The advantage is that it captures
 621 the zero potential vorticity of the angular momentum conserving circulation in a nat-
 622 ural way (Held & Hou, 1980). Meanwhile, latent heat release from carbon dioxide de-
 623 position over the winter pole alters the polar potential vorticity (Toigo et al., 2017) and
 624 the effects of the two processes on the annular distribution can be analyzed in isolation.

625 Moving towards more complex models, a large number of studies have investigated
 626 polar vortices in stratified atmospheres using three-dimensional integrations of the prim-
 627 itive equations (Figure 7e). In their simplest form, these consist of a Newtonian ther-
 628 mal relaxation towards a specified temperature profile, in place of an explicit represen-
 629 tation of radiation (Held & Suarez, 1994). Such relaxation schemes have been adapted
 630 for application to Earth’s polar stratosphere (Polvani & Kushner, 2002; Jucker et al., 2014)
 631 and are able to capture a realistic vortex climatology, as well as both split and displace-
 632 ment sudden stratospheric warming events (Gerber & Polvani, 2009). By varying sur-
 633 face topographic and surface heating forcings, as well as lower-stratospheric winds, within
 634 such simulations, studies have made progress in explaining the observed seasonality and
 635 inter-hemispheric differences in the frequency of sudden stratospheric warmings (Sheshadri
 636 et al., 2015; Martineau et al., 2018; Lindgren et al., 2018; Scott & Polvani, 2006). Sim-
 637 ilar Newtonian relaxation schemes have been applied to the atmospheres of Venus (Yamamoto
 638 & Takahashi, 2006; Lee et al., 2007, 2010), with Lee et al. (2010) in particular simulat-

639 ing the hemispheric polar vortex and associated spiral arms seen in observations, and
 640 Mars (Collins & James, 1995; Haberle et al., 1997; Thomson & Vallis, 2019b), with the
 641 addition of a temperature lower bound to represent CO_2 condensation. While these stud-
 642 ies produced relatively realistic polar zonal winds, they have not focused in detail on po-
 643 lar vortex structure.

644 At the top of the hierarchy of model complexity sit comprehensive general circula-
 645 tion models (GCMs; Figure 7f), which include both a radiation scheme, parameteri-
 646 sations for subgrid-scale processes such as convection and clouds, and possibly a coupled
 647 ocean and interactive atmospheric chemistry. In recent years many Earth GCMs have
 648 moved towards increased vertical resolution in the stratosphere, leading to an improve-
 649 ment in their representation of the stratospheric polar vortex and its variability (Charlton-
 650 Perez et al., 2013). Despite this, there remain longstanding biases including too few sud-
 651 den stratospheric warming events in most models (Charlton & Polvani, 2007), as well
 652 as an underestimate of the relative frequency of split vortex (or zonal wavenumber-2)
 653 events (Seviour et al., 2016) (though it should be noted that biases vary widely between
 654 models). Importantly, GCMs are used to understand how vortex variability may vary
 655 under climate change, an area of research where great uncertainty remains (see Baldwin
 656 et al. (2020), for a detailed discussion). Some Martian GCMs include comprehensive rep-
 657 resentations of the global dust cycle and dust aerosol properties, with many GCMs able
 658 to simulate prescribed or freely-evolving dust storms, and CO_2 condensation which both
 659 play significant roles in polar vortex dynamics, as discussed in Section 3. Indeed, Toigo
 660 et al. (2017) showed that if the process of CO_2 condensation is turned off in their GCM,
 661 the vortex took on a monopolar, rather than annular PV structure, and so argued that
 662 it is this process which leads to the observed annulus. Ball et al. (2021) showed that with
 663 the inclusion of dust in an idealized Martian GCM the mean-state and variability of the
 664 northern Martian polar vortex were significantly better captured. Titan GCMs have been
 665 developed to include a representation of the methane cycle (Lora et al., 2015), and have
 666 been applied to simulate the tropospheric and stratospheric circulations, though mod-
 667 elling studies have not focussed explicitly on polar vortex structure. There are, in ad-
 668 dition, great uncertainties when comparing existing Titan GCMs (Lora et al., 2019; Lebon-
 669 nois et al., 2012), particularly in the strength of extratropical zonal winds and the de-
 670 gree of superrotation (Newman et al., 2011). Continued improvement in the simulation
 671 of planetary polar vortices will necessitate more detailed inclusion of important phys-
 672 ical processes in GCMs, while at the same time gaining physical insight and understand-
 673 ing from the use of more idealised models.

674 5 Polar vortices in the laboratory

675 Laboratory studies provide an alternative type of model which complements those
 676 discussed in Section 4 (Figure 7c). Perhaps the most common type of laboratory study
 677 concerned with large-scale atmospheric dynamics is the thermally-driven rotating an-
 678 nulus experiment, on which there is a vast literature that we do not completely review
 679 here, where a rotating cylinder of fluid is cooled at the inner boundary and heated at
 680 the outer boundary, representing the differential heating of a planet by its star (e.g. (Hide,
 681 1953; Fultz et al., 1959)). Thermally-driven rotating annulus experiments have mostly
 682 been concerned with studying regimes of baroclinically unstable situations, perhaps most
 683 relevant to midlatitude on Earth and other planets. For example, transitions are typ-
 684 ically observed from axisymmetric overturning Hadley-cells, through weakly-nonlinear
 685 wave-like regimes to full geostrophic turbulence with multiple jets as parameters are changed
 686 (e.g. (Hide & Mason, 1970; Hart, 1972; Hide & Mason, 1975; Spence & Fultz, 1977; Bastin
 687 & Read, 1998; Read, 2011)). Such baroclinic-wave-like behaviour and interactions with
 688 the overturning circulation are perhaps most relevant for polar vortices like those on Mars,
 689 whose baroclinic wave-like behaviour has been compared with the wave-like regimes in
 690 rotating annuli (Collins & James, 1995), although there are certainly parallels to be drawn

691 between the wave dynamics observed in annulus experiments, and the waves typically
 692 found on the polar vortex edge on Earth. One weakness of using such experiments for
 693 studies of polar vortices specifically is that they necessarily contain some kind of cen-
 694 tral barrier near the axis of rotation (normally used to contain a source of cooling to drive
 695 horizontal motion within the annulus). Such a barrier therefore prevents a vortex form-
 696 ing right over the pole. Experiments forced in other ways can remove the need for such
 697 a central column, and thus study jet formation and polar vortex formation in polar re-
 698 gions. One particular example of this is the experiment of (Y. Afanasyev & Wells, 2005),
 699 which is a rectangular rotating tank with a cylindrical insert, and is forced by an initial
 700 array of vortex dipoles created through the combination of electrical currents and an ar-
 701 ray of magnets. Such a setup is found to produce circumpolar jet streams, and displays
 702 a PV maximum over the pole, and a wavy jet edge, somewhat reminiscent of a typical
 703 Type I vortex (see e.g. figure 2a of (Y. Afanasyev & Wells, 2005)). Varying the rotation
 704 rate of such an experiment allows vortex properties to be compared across different regimes,
 705 with smaller values of β producing a more isotropic region of chaotically-interacting cir-
 706 cular vortices. For a more general discussion of experiments of this kind, see (Y. D. Afanasyev,
 707 2019).

708 For planets where the thermally-driven meridional overturning circulation is not
 709 connected to the polar vortex, e.g. those on the giant planets, the thermally-driven an-
 710 nulus experiments are perhaps less relevant. There are a relatively small number of stud-
 711 ies, however, that have investigated such polar vortices in laboratory experiments. A key
 712 example is the study of Saturn’s polar hexagon (Aguiar et al., 2010) (see also Figure 7c),
 713 with other more generalised examples also providing relevant insight (Montabone, Wordsworth,
 714 Aguiar, Jacoby, Read, et al., 2010; Montabone, Wordsworth, Aguiar, Jacoby, Manfrin,
 715 et al., 2010). These studies use rotating tanks without any differential heating. They are
 716 based on the idea that the wave-like polygonal shapes around polar vortices are a man-
 717 ifestation of barotropic instability. Others have used a differentially rotating section of
 718 their tank’s upper lid to spin up a barotropically unstable jet (Aguiar et al., 2010). They
 719 find regimes where wave-like perturbations are superposed on the jet, which saturate at
 720 finite amplitude, with the wavenumber of the perturbation depending on their param-
 721 eters. Although they cannot approach Saturnian parameters with all of their control pa-
 722 rameters, a Saturn-like Rossby number can be attained, and this regime shows a pref-
 723 erence for hexagonal wave-6 waves. Similar results have also been found in other stud-
 724 ies (Montabone, Wordsworth, Aguiar, Jacoby, Read, et al., 2010; Montabone, Wordsworth,
 725 Aguiar, Jacoby, Manfrin, et al., 2010), but in a setup where their vortex is created by
 726 having a sink of fluid over the centre of their tank. They also find low-wavenumber per-
 727 turbations to the vortices that share some similarities with perturbations seen on Earth,
 728 Venus and Saturn. More recent numerical work has suggested that perhaps the presence
 729 of a polar vortex over the pole is important to produce a more Saturn-like hexagon than
 730 is produced in these lab experiments (Rostami et al., 2017), but in essence the paper high-
 731 lights the same mechanism - namely that barotropic instability is able to generate the
 732 hexagonal pattern.

733 One weakness, perhaps, of past laboratory experiments studying polar vortices on
 734 giant planets is that they do not readily include the poleward migration of small vor-
 735 tices that may be relevant for forming polar vortices (as described in section 4). To in-
 736 clude such effects in a lab experiment would require the representation of the β effect,
 737 and a mechanism for producing small vortices. As is well-known, the β effect can be rep-
 738 resented through the use of either a sloping bottom boundary (when using a fixed-upper
 739 lid), or by utilising the parabolic shape adopted by a rotating mass of fluid with a free
 740 upper surface. It is possible to represent small-scale moist convection in lab experiments
 741 using saline injections (e.g. (Read et al., 2004)), vertical forcing through the use of mag-
 742 nets (e.g. (Y. Afanasyev & Wells, 2005)), and of course small vortices can be generated
 743 through thermally-driven convection (e.g. in rotating annuli). Perhaps one future direc-
 744 tion for laboratory experiments relating to polar vortices would be to attempt to rep-

745 resent both the barotropic-instability of polar jet streams and the poleward migration
 746 of small vortices, with the hope that the interaction of these mechanisms could be bet-
 747 ter understood.

748 A significant insight gained from laboratory experiments is the utility of regime di-
 749 agrams, which are commonly used to describe the flow behaviour as a function of pa-
 750 rameters in laboratory experiments (Read, 2011). These have recently proved insight-
 751 ful when describing regimes of behaviour in global circulation model experiments using
 752 non-dimensional (Wang et al., 2018; Thomson & Vallis, 2019a), or dimensional param-
 753 eters (Kaspi & Showman, 2015; Komacek & Abbot, 2019). As studies of planetary polar
 754 vortices are extended to wider parameter ranges, such regime diagrams may also prove
 755 useful for understanding polar vortex behaviours over a range of planetary attributes.

756 6 Thinking beyond our solar system

757 Given that over 4000 exoplanets have been discovered to date, many with substan-
 758 tial atmospheres (NASA Exoplanet Archive: doi:10.26133/NEA1), the polar vortices in
 759 our solar system are likely to represent only a small subset of polar vortices that could
 760 exist in a planetary atmosphere. If Earth were an exoplanet, our current infrared mea-
 761 surements would observe the upper atmosphere, namely the stratosphere and mesosphere,
 762 but not the troposphere. Polar circulations in these regions are particularly important
 763 because they can redistribute atmospheric constituents, depending on how stable they
 764 are. Observation-based estimates of the zonal wind speed for planetary bodies outside
 765 the solar system exist, for instance, on brown dwarfs, which are hypothesised to have po-
 766 lar vortex-dominated regimes (Apai et al., 2021). By comparing the period of the infrared
 767 emissions from the upper atmosphere, with the period of the radio emissions from the
 768 planet interior, Allers et al. (2020) estimated that their chosen brown dwarf had strong
 769 westerlies of $650 \pm 310 \text{ ms}^{-1}$, although subsequent modelling studies have not been able
 770 to capture the magnitude of these winds (Tan & Showman, 2021).

771 Due to the nature of the detection methods used, the known exoplanets are nor-
 772 mally very close to their parent star and have very fast orbital periods, often equivalent
 773 to 5-35 Earth days. One consequence of this is that tidal forces are stronger, often re-
 774 sulting in the planetary rotation rate and orbital periods synchronising, which puts their
 775 atmospheres into very different regimes than those observed in our solar system. These
 776 are known as tidally locked regimes, and the majority of exoplanet atmospheric dynam-
 777 ics studies have focussed on this regime type.

778 To date, there have been no targeted studies modelling polar vortices on exoplanets
 779 but there have been a number of studies looking at other features of planetary at-
 780 mospheric circulation, notably either atmospheric winds in a general sense, or the Hadley
 781 circulation which is a controlling factor for some polar vortices. In the context of exo-
 782 planets, these studies generally fall into two categories. The first are targeted studies of
 783 a specific exoplanet atmosphere. The most common systems studied are TRAPPIST and
 784 Proxima Centuri, as those have been some of the most observed and have high chances
 785 of Earth-like planets. While not all necessary atmospheric boundary conditions to run
 786 GCMs of exoplanets are yet measurable, Fauchez et al. (2020) modelled the atmospheric
 787 circulation of TRAPPIST-1e using plausible assumptions of the unknown parameters.
 788 Here we show their data re-plotted to focus on the polar region (Figure 9), where a po-
 789 lar vortex with strong zonal winds ($50\text{-}60 \text{ ms}^{-1}$) exists, with cold polar temperatures,
 790 much like some of the vortices described in Section 3. However, polar vortices do not al-
 791 ways exist, and Carone et al. (2015) showed that polar tropospheric jets were possible
 792 for some tidally locked planets with specific planetary parameters. However, these did
 793 not exist on planets with longer orbital periods, in which cases radial flow dominated over
 794 the zonal flows. The relationship is more apparent for larger planets, for instance some
 795 of those in the Proxima Centuri system. Expanding on their earlier work, Carone et al.

796 (2018) specifically look at the stratospheric circulation on exoplanets within the TRAP-
 797 PIST and Proxima Centuri, and identify weak polar jets in both hemispheres at the same
 798 time, but only when the stratospheric overturning circulation was dominated by extra-
 799 tropical vertical Rossby wave activity. If instead it is dominated by tropical wave activ-
 800 ity, the jets were not established.

801 The second category of exoplanetary analysis is focussed more on the idealised na-
 802 ture of atmospheric regimes to changes in planetary parameters, such as the planetary
 803 rotation rate, or planetary radius, rather than modelling a specific exoplanet. These stud-
 804 ies consider both tidally locked, and freely rotating exoplanets, and show in both cases
 805 that tropospheric jets can form in the polar regions for Earth-sized exoplanets (Edson
 806 et al., 2011). Again, these studies do not explicitly focus on the polar vortices, but we
 807 can infer some characteristics from other circulation diagnostics. For instance, a body
 808 of research shows that the width of the Hadley cell has a strong dependence on the plan-
 809 etary rotation rate and radius, with the cell extending further poleward for slower ro-
 810 tating planets, or smaller radii planets (Held & Hou, 1980; Kaspi & Showman, 2015; Ko-
 811 macek & Abbot, 2019). The atmospheric cloud particle size has a secondary effect, with
 812 larger particles giving rise to a more vigorous atmospheric circulation, which will be es-
 813 pecially important for planets with convectively active polar vortices, such as the solar
 814 system gas-giants (Komacek & Abbot, 2019). The atmospheric mass of the planet is an-
 815 other key parameter that is strongly correlated with the strength of the Hadley Cell, with
 816 thicker atmospheres giving rise to stronger poleward transport (Chemke & Kaspi, 2017).

817 Importantly, almost all studies of exoplanet atmospheric circulation have focussed
 818 on equinox conditions. However, as we have discussed in Sections 1-4, many polar vor-
 819 tices have strong seasonal dependence, existing only from autumn until spring. There
 820 is a clear need, therefore, for understanding the solstice and seasonally-varying proper-
 821 ties of exoplanet atmospheric circulation.

822 Considering the vast numbers of planetary parameters that have a controlling in-
 823 fluence on atmospheric dynamics (Kaspi & Showman, 2015; Guendelman & Kaspi, 2018;
 824 Read et al., 2018; Wang et al., 2018; Komacek & Abbot, 2019; Thomson & Vallis, 2019a),
 825 it is likely that polar vortex dynamical regimes exist that are far beyond what we have
 826 yet imagined.

827 **7 Summary and Outlook**

828 In this review, building on research from the 1800s to the present day, we have in-
 829 dicated how the observed genesis and structure of planetary polar vortices can be un-
 830 derstood in terms of 1) basic planetary parameters which control the freely-evolving large-
 831 scale circulation, such as planetary rotation rate or atmospheric stratification, 2) global
 832 forcings such as solar forcing and obliquity, and 3) local forcing processes, such as the
 833 Martian latent heating from the condensation of atmospheric constituents. Within this
 834 framework, and the wider literature discussed throughout the review, we note the fol-
 835 lowing key challenges for planetary polar vortex research in the future:

- 836 • To what extent do forcing asymmetries alter the structure of polar vortices? The
 837 largest unknowns come in the local forcings, and in some cases the forcings, such
 838 as the nature and organisation of convection on gas giants are not necessarily known
 839 (Dyudina et al., 2008; Thomson & McIntyre, 2016).
- 840 • What determines if a planet will have a polar vortex of Type I or II? Understand-
 841 ing what forcing mechanisms in a system can lead to multiple vortex configura-
 842 tions could in the future point to possible explanations of the vortex structures
 843 observed at Jupiter’s poles, for instance. Understanding of how the various mech-
 844 anisms interact with each other, perhaps as a function of planetary parameters,
 845 is a related and important step in understanding this question.

- 846 • What are the stabilising forces of the annular polar vortices for the planets that
847 have them? Such structures are clear on Mars, and Titan, although the exact sta-
848 bilising mechanisms are still unknown. The degree to which the Venusian polar
849 vortex is annular is still debated.
- 850 • What is the role of atmospheric composition in defining vortex structure and evo-
851 lution? This could be in terms of the effect of local gas enrichments on radiative
852 forcing as in the case of Titan (Teanby et al., 2017), or condensation of major species
853 providing a latent heat source as in the case of Mars (Toigo et al., 2017). Dynam-
854 ical redistribution of trace species by the circulation means such processes may
855 also play a role in the giant planets. It is therefore important to consider such ef-
856 fects in future GCMs.
- 857 • How far below the cloud top do the polar vortices extend in gas planets? This is
858 even unknown for Saturn and Jupiter, where we have much greater coverage of
859 their polar atmospheres. Focusing on convection processes in our comprehensive
860 models will likely shed light in this area.
- 861 • Can exoplanet observations and modelling of polar vortices combine to help both
862 communities? Some (highly uncertain) observation-derived estimates for zonal wind
863 speeds on exoplanets exist, but in the coming decades these will increase in quan-
864 tity and quality. Using theory and modelling to identify potential planets of in-
865 terest will help inform observers as to where to look. In turn, better observations
866 help improve our overall theories of polar vortex dynamics.
- 867 • What other types of polar vortex could exist in the exotic atmospheres outside
868 our solar system? While there have been some studies where different planetary
869 parameters, and scaling relationships, have been iterated to understand how fea-
870 tures of polar vortices and jets depend on them (e.g. Brueshaber et al. (2019); Guen-
871 delman and Kaspi (2018)), there remains a wide parameter-space that exoplan-
872 ets could exist in, and that could provide a deeper understanding of the atmospheric
873 dynamics. Given the utility of regime diagrams for understanding dependence on
874 parameters, we suggest that creation of regime diagrams for polar vortices be a
875 priority for future research, showing how the properties of the vortex can be un-
876 derstood in terms of dimensional and non-dimensional planetary parameters.

877 Beyond this, there is now a clear need to place our understanding of polar vortices
878 and their governing processes, developed for individual solar system planets, into a sin-
879 gle dynamical framework along the lines of the three categories presented at the begin-
880 ning of this summary. This is especially true now given the rapidly-increasing volume
881 of exoplanetary data, that will be further enhanced by imminent new exoplanet-focused
882 initiatives, such as the James Webb Space Telescope.

883 References

- 884 Achterberg, R. K., Conrath, B. J., Gierasch, P. J., Flasar, F. M., & Nixon, C. A.
885 (2008). Titan’s middle-atmospheric temperatures and dynamics observed by
886 the Cassini Composite Infrared Spectrometer. *Icarus*, *194*(1), 263–277.
- 887 Achterberg, R. K., Gierasch, P. J., Conrath, B. J., Flasar, F. M., & Nixon, C. A.
888 (2011). Temporal variations of Titan’s middle-atmospheric temperatures
889 from 2004 to 2009 observed by Cassini/CIRS. *Icarus*, *211*, 686 - 698. doi:
890 10.1016/j.icarus.2010.08.009
- 891 Adriani, A., Mura, A., Orton, G., Hansen, C., Altieri, F., Moriconi, M., ... others
892 (2018). Clusters of cyclones encircling Jupiter’s poles. *Nature*, *555*(7695), 216.
- 893 Afanasyev, Y., & Wells, J. (2005, feb). Quasi-two-dimensional turbulence on the pol-
894 ar beta-plane: laboratory experiments. *Geophysical & Astrophysical Fluid Dy-*
895 *namics*, *99*(1), 1–17. Retrieved from [http://www.tandfonline.com/doi/abs/](http://www.tandfonline.com/doi/abs/10.1080/03091920412331319513)
896 [10.1080/03091920412331319513](http://www.tandfonline.com/doi/abs/10.1080/03091920412331319513) doi: 10.1080/03091920412331319513
- 897 Afanasyev, Y. D. (2019, feb). Turbulence, Rossby Waves and Zonal Jets on

- 898 the Polar β -Plane: Experiments with Laboratory Altimetry. In *Zonal jets*
 899 (Vol. 2, pp. 152–166). Cambridge University Press. Retrieved from [https://](https://www.cambridge.org/core/product/identifier/9781107358225/%23c8/type/book/_part)
 900 [www.cambridge.org/core/product/identifier/9781107358225/%23c8/](https://www.cambridge.org/core/product/identifier/9781107358225/%23c8/type/book/_part)
 901 [type/book/_part](https://www.cambridge.org/core/product/identifier/9781107358225/%23c8/type/book/_part) doi: 10.1017/9781107358225.008
- 902 Aguiar, A. C. B., Read, P. L., Wordsworth, R. D., Salter, T., & Yamazaki, Y. H.
 903 (2010). A laboratory model of Saturn’s north polar hexagon. *Icarus*, *206*(2),
 904 755–763.
- 905 Allers, K. N., Vos, J. M., Biller, B. A., & Williams, P. K. (2020). A measurement of
 906 the wind speed on a brown dwarf. *Science*, *368*(6487), 169–172.
- 907 Allison, M., Godfrey, D., & Beebe, R. (1990). A wave dynamical interpretation of
 908 Saturn’s polar hexagon. *Science*, *247*(4946), 1061–1063.
- 909 Andrews, D., Holton, J. R., & Leovy, C. (1987). *Middle Atmosphere Dynamics*. San
 910 Diego, Calif.: Academic Press.
- 911 Andrews, D. G. (1987). On the interpretation of the Eliassen–Palm flux divergence.
 912 *Quarterly Journal of the Royal Meteorological Society*, *113*(475), 323–338.
- 913 Antuñano, A., del Río-Gaztelurrutia, T., Sánchez-Lavega, A., & Hueso, R. (2015).
 914 Dynamics of Saturn’s polar regions. *Journal of Geophysical Research: Planets*,
 915 *120*(2), 155–176.
- 916 Antuñano, A., del Río-Gaztelurrutia, T., Sánchez-Lavega, A., Read, P. L., &
 917 Fletcher, L. N. (2019). Potential vorticity of Saturn’s polar regions: Sea-
 918 sonality and instabilities. *Journal of Geophysical Research: Planets*, *124*(1),
 919 186–201.
- 920 Antuñano, A., del Río-Gaztelurrutia, T., Sánchez-Lavega, A., & Rodríguez-
 921 Aseguinolaza, J. (2018). Cloud morphology and dynamics in Saturn’s northern
 922 polar region. *Icarus*, *299*, 117–132.
- 923 Apai, D., Nardiello, D., & Bedin, L. R. (2021). Tess observations of the Luhman 16
 924 ab brown dwarf system: Rotational periods, lightcurve evolution, and zonal
 925 circulation. *The Astrophysical Journal*, *906*(1), 64.
- 926 Baines, K. H., Momary, T. W., Fletcher, L. N., Showman, A. P., Roos-Serote, M.,
 927 Brown, R. H., . . . Nicholson, P. D. (2009). Saturn’s north polar cyclone and
 928 hexagon at depth revealed by Cassini/VIMS. *Planetary and Space Science*,
 929 *57*(14–15), 1671–1681.
- 930 Baldwin, M. P., Ayarzagüena, B., Birner, T., Butchart, N., Butler, A. H., Charlton-
 931 Perez, A. J., . . . others (2020). Sudden stratospheric warmings. *Reviews of*
 932 *Geophysics*, e2020RG000708.
- 933 Baldwin, M. P., & Dunkerton, T. J. (2001). Stratospheric harbingers of anomalous
 934 weather regimes. *Science*, *294*(5542), 581–584.
- 935 Ball, E. R., Mitchell, D. M., Seviour, W. J., Thomson, S. I., & Vallis, G. K. (2021).
 936 The roles of latent heating and dust in the structure and variability of the
 937 northern martian polar vortex. *Planetary Science Journal*, *Accepted*. doi:
 938 10.3847/PSJ/ac1ba2
- 939 Banfield, D., Conrath, B., Gierasch, P., John Wilson, R., & Smith, M. (2004). Trav-
 940 eling waves in the martian atmosphere from MGS TES nadir data. *Icarus*,
 941 *170*, 365 - 403. doi: 10.1016/j.icarus.2004.03.015
- 942 Bastin, M. E., & Read, P. L. (1998, feb). Experiments on the structure of baroclinic
 943 waves and zonal jets in an internally heated, rotating, cylinder of fluid. *Physics*
 944 *of Fluids*, *10*(2), 374–389. Retrieved from [http://aip.scitation.org/doi/](http://aip.scitation.org/doi/10.1063/1.869530)
 945 [10.1063/1.869530](http://aip.scitation.org/doi/10.1063/1.869530) doi: 10.1063/1.869530
- 946 Bolton, S. J., Adriani, A., Adumitroaie, V., Allison, M., Anderson, J., Atreya, S., . . .
 947 others (2017). Jupiter’s interior and deep atmosphere: The initial pole-to-pole
 948 passes with the Juno spacecraft. *Science*, *356*(6340), 821–825.
- 949 Brueshaber, S. R., Sayanagi, K. M., & Dowling, T. E. (2019). Dynamical regimes of
 950 giant planet polar vortices. *Icarus*, *323*, 46–61.
- 951 Butler, A. H., Sjöberg, J. P., Seidel, D. J., & Rosenlof, K. H. (2017). A sudden
 952 stratospheric warming compendium. *Earth System Science Data*, *9*(1).

- 953 Cantor, B. A., James, P. B., Caplinger, M., & Wolff, M. J. (2001). Martian dust
954 storms: 1999 Mars Orbiter Camera observations. *Journal of Geophysical*
955 *Research: Planets*, 106(E10), 23653-23687. Retrieved from [https://](https://agupubs.onlinelibrary.wiley.com/doi/abs/10.1029/2000JE001310)
956 agupubs.onlinelibrary.wiley.com/doi/abs/10.1029/2000JE001310 doi:
957 <https://doi.org/10.1029/2000JE001310>
- 958 Carone, L., Keppens, R., & Decin, L. (2015). Connecting the dots—ii. phase changes
959 in the climate dynamics of tidally locked terrestrial exoplanets. *Monthly No-*
960 *tices of the Royal Astronomical Society*, 453(3), 2412–2437.
- 961 Carone, L., Keppens, R., Decin, L., & Henning, T. (2018). Stratosphere circulation
962 on tidally locked exoearths. *Monthly Notices of the Royal Astronomical Soci-*
963 *ety*, 473(4), 4672–4685.
- 964 Charlton, A. J., & Polvani, L. M. (2007). A new look at stratospheric sudden
965 warmings. part i: Climatology and modeling benchmarks. *Journal of Climate*,
966 20(3), 449–469.
- 967 Charlton-Perez, A. J., Baldwin, M. P., Birner, T., Black, R. X., Butler, A. H.,
968 Calvo, N., ... others (2013). On the lack of stratospheric dynamical variability
969 in low-top versions of the cmip5 models. *Journal of Geophysical Research:*
970 *Atmospheres*, 118(6), 2494–2505.
- 971 Charney, J. G., & Drazin, P. G. (1961). Propagation of planetary-scale disturbances
972 from the lower into the upper atmosphere. *Journal of Geophysical Research*,
973 66(1), 83–109.
- 974 Chemke, R., & Kaspi, Y. (2017). Dynamics of massive atmospheres. *The Astrophys-*
975 *ical Journal*, 845(1), 1.
- 976 Collins, M., & James, I. (1995). Regular baroclinic transient waves in a simpli-
977 fied global circulation model of the martian atmosphere. *Journal of Geophysi-*
978 *cal Research: Planets*, 100(E7), 14421–14432.
- 979 Coustenis, A., Jennings, D. E., Achterberg, R. K., Lavvas, P., Bampasidis, G.,
980 Nixon, C. A., & Flasar, F. M. (2020, July). Titan’s neutral atmosphere
981 seasonal variations up to the end of the Cassini mission. *Icarus*, 344, 113413.
982 doi: 10.1016/j.icarus.2019.113413
- 983 de Pater, I., Fletcher, L. N., Luszcz-Cook, S., DeBoer, D., Butler, B., Ham-
984 mel, H. B., ... Marcus, P. S. (2014). Neptune’s global circulation de-
985 duced from multi-wavelength observations. *Icarus*, 237, 211-238. doi:
986 10.1016/j.icarus.2014.02.030
- 987 Deem, G. S., & Zabusky, N. J. (1978). Vortex waves: Stationary” v states,” interac-
988 tions, recurrence, and breaking. *Physical Review Letters*, 40(13), 859.
- 989 de Kok, R. J., Teanby, N. A., Maltagliati, L., Irwin, P. G., & Vinatier, S. (2014).
990 HCN ice in Titan’s high-altitude southern polar cloud. *Nature*, 514(7520), 65.
- 991 de Pater, I., Sromovsky, L., Fry, P., Hammel, H. B., Baranec, C., & Sayanagi, K. M.
992 (2015). Record-breaking storm activity on Uranus in 2014. *Icarus*, 252,
993 121–128.
- 994 Domeisen, D. I. V., & Butler, A. H. (2020, December). Stratospheric drivers of ex-
995 treme events at the Earth’s surface. *Communications Earth and Environment*,
996 1(1), 59. doi: 10.1038/s43247-020-00060-z
- 997 Dritschel, D. G. (1986). The nonlinear evolution of rotating configurations of uni-
998 form vorticity. *Journal of Fluid Mechanics*, 172, 157–182.
- 999 Dritschel, D. G., & Polvani, L. M. (1992). The roll-up of vorticity strips
1000 on the surface of a sphere. *J. Fluid Mech.*, 234, 47–69. doi: 10.1017/
1001 S0022112092000697
- 1002 Dyudina, U. A., Ingersoll, A. P., Ewald, S. P., Vasavada, A. R., West, R. A., Baines,
1003 K. H., ... others (2009). Saturn’s south polar vortex compared to other large
1004 vortices in the solar system. *Icarus*, 202(1), 240–248.
- 1005 Dyudina, U. A., Ingersoll, A. P., Ewald, S. P., Vasavada, A. R., West, R. A., Del Ge-
1006 nio, A. D., ... others (2008). Dynamics of Saturn’s south polar vortex.
1007 *Science*, 319(5871), 1801–1801.

- 1008 Edson, A., Lee, S., Bannon, P., Kasting, J. F., & Pollard, D. (2011). Atmospheric
1009 circulations of terrestrial planets orbiting low-mass stars. *Icarus*, *212*(1),
1010 1–13.
- 1011 Farman, J. C., Gardiner, B. G., & Shanklin, J. D. (1985). Large losses of total ozone
1012 in antarctica reveal seasonal clox/nox interaction. *Nature*, *315*(6016), 207.
- 1013 Fauchez, T. J., Turbet, M., Wolf, E. T., Boutle, I., Way, M. J., Del Genio, A. D.,
1014 ... others (2020). Trappist-1 habitable atmosphere intercomparison (thai).
1015 motivations and protocol version 1.0. *arXiv preprint arXiv:2002.10950*.
- 1016 Fine, K., Cass, A., Flynn, W., & Driscoll, C. (1995). Relaxation of 2d turbulence to
1017 vortex crystals. *Physical review letters*, *75*(18), 3277.
- 1018 Flasar, F., & Achterberg, R. (2008). The structure and dynamics of Titan’s middle
1019 atmosphere. *Philosophical Transactions of the Royal Society A: Mathematical,*
1020 *Physical and Engineering Sciences*, *367*(1889), 649–664.
- 1021 Flasar, F. M., Kunde, V. G., Abbas, M. M., Achterberg, R. K., Ade, P., Barucci, A.,
1022 ... Taylor, F. W. (2004). Exploring the Saturn system in the thermal infrared:
1023 The Composite Infrared Spectrometer. *Space Science Reviews*, *115*, 169–297.
- 1024 Fletcher, L., Irwin, P., Orton, G., Teanby, N., Achterberg, R., Bjoraker, G., ... oth-
1025 ers (2008). Temperature and composition of Saturn’s polar hot spots and
1026 hexagon. *Science*, *319*(5859), 79–81.
- 1027 Fletcher, L. N., Hesman, B., Achterberg, R., Irwin, P., Bjoraker, G., Gorius, N., ...
1028 others (2012). The origin and evolution of Saturn’s 2011–2012 stratospheric
1029 vortex. *Icarus*, *221*(2), 560–586.
- 1030 Fletcher, L. N., Irwin, P., Sinclair, J., Orton, G., Giles, R., Hurley, J., ... Bjoraker,
1031 G. (2015). Seasonal evolution of Saturn’s polar temperatures and composition.
1032 *Icarus*, *250*, 131–153.
- 1033 Fletcher, L. N., Orton, G. S., Sinclair, J. A., Guerlet, S., Read, P. L., Antuñano,
1034 A., ... Calcutt, S. B. (2018, September). A hexagon in Saturn’s northern
1035 stratosphere surrounding the emerging summertime polar vortex. *Nature*
1036 *Communications*, *9*, 3564. doi: 10.1038/s41467-018-06017-3
- 1037 Fultz, D., Long, R. R., Owens, G. V., Bohan, W., Kaylor, R., & Weil, J. (1959).
1038 Studies of thermal convection in a rotating cylinder with some implications for
1039 large-scale atmospheric motions. In *Studies of thermal convection in a rotat-*
1040 *ing cylinder with some implications for large-scale atmospheric motions* (pp.
1041 1–104). Springer.
- 1042 Garate-Lopez, I., Hueso, R., Sánchez-Lavega, A., & García Muñoz, A. (2016). Po-
1043 tential vorticity of the south polar vortex of Venus. *Journal of Geophysical Re-*
1044 *search: Planets*, *121*(4), 574–593.
- 1045 Garate-Lopez, I., Hueso, R., Sánchez-Lavega, A., Peralta, J., Piccioni, G., &
1046 Drossart, P. (2013). A chaotic long-lived vortex at the southern pole of
1047 Venus. *Nature Geoscience*, *6*(4), 254.
- 1048 Garate-Lopez, I., Muñoz, A. G., Hueso, R., & Sánchez-Lavega, A. (2015). Instanta-
1049 neous three-dimensional thermal structure of the south polar vortex of Venus.
1050 *Icarus*, *245*, 16–31.
- 1051 Gerber, E. P., & Polvani, L. M. (2009). Stratosphere–troposphere coupling in a rela-
1052 tively simple agcm: The importance of stratospheric variability. *Journal of Cli-*
1053 *mate*, *22*(8), 1920–1933.
- 1054 Gierasch, P., Goody, R., Young, R., Crisp, D., Edwards, C., Kahn, R., ... others
1055 (1997). The general circulation of the Venus atmosphere: An assessment.
1056 *Venus II*, 459–500.
- 1057 Godfrey, D. A. (1988). A hexagonal feature around Saturn’s north pole. *Icarus*,
1058 *76*(2), 335–356. doi: 10.1016/0019-1035(88)90075-9
- 1059 Greybush, S. J., Wilson, R. J., Hoffman, R. N., Hoffman, M. J., Miyoshi, T., Ide, K.,
1060 ... Kalnay, E. (2012). Ensemble Kalman filter data assimilation of Thermal
1061 Emission Spectrometer temperature retrievals into a Mars GCM. *J. Geophys.*
1062 *Res. Planets*, *117*, E11008. doi: 10.1029/2012JE004097

- 1063 Guendelman, I., & Kaspi, Y. (2018). An axisymmetric limit for the width of the
1064 hadley cell on planets with large obliquity and long seasonality. *Geophysical*
1065 *Research Letters*, *45*(24), 13–213.
- 1066 Gutenberg, B. (1949). New data on the lower stratosphere. *Bulletin of the American*
1067 *Meteorological Society*, *30*(2), 62–64.
- 1068 Guzewich, S. D., Toigo, A., & Waugh, D. (2016). The effect of dust on the martian
1069 polar vortices. *Icarus*, *278*, 100 - 118. doi: 10.1016/j.icarus.2016.06.009
- 1070 Haberle, R. M., Clancy, R. T., Forget, F., Smith, M. D., & Zurek, R. W. (2017).
1071 *The atmosphere and climate of mars*. Cambridge University Press.
- 1072 Haberle, R. M., Houben, H., Barnes, J. R., & Young, R. E. (1997). A simplified
1073 three-dimensional model for martian climate studies. *Journal of Geophysical*
1074 *Research: Planets*, *102*(E4), 9051–9067.
- 1075 Hart, J. E. (1972, may). A laboratory study of baroclinic instability. *Geo-*
1076 *physical Fluid Dynamics*, *3*(3), 181–209. Retrieved from [https://](https://www.tandfonline.com/doi/full/10.1080/03091927208236080)
1077 www.tandfonline.com/doi/full/10.1080/03091927208236080 doi:
1078 10.1080/03091927208236080
- 1079 Haynes, P., & McIntyre, M. (1990). On the conservation and impermeability theo-
1080 rems for potential vorticity. *Journal of the atmospheric sciences*, *47*(16), 2021–
1081 2031.
- 1082 Held, I. M., & Hou, A. Y. (1980). Nonlinear axially symmetric circulations in a
1083 nearly inviscid atmosphere. *Journal of the Atmospheric Sciences*, *37*(3), 515–
1084 533.
- 1085 Held, I. M., & Suarez, M. J. (1994). A proposal for the intercomparison of the dy-
1086 namical cores of atmospheric general circulation models. *Bulletin of the Amer-*
1087 *ican Meteorological Society*, *75*(10), 1825 - 1830. doi: 10.1175/1520-0477(1994)
1088 075<1825:APFTIO>2.0.CO;2
- 1089 Hide, R. (1953). Some experiments on thermal convection in a rotating liquid. *Quar-*
1090 *terly Journal of the Royal Meteorological Society*, *79*(339), 161–161.
- 1091 Hide, R., & Mason, P. (1970, nov). Baroclinic waves in a rotating fluid subject to
1092 internal heating. *Philosophical Transactions of the Royal Society of London.*
1093 *Series A, Mathematical and Physical Sciences*, *268*(1186), 201–232. Retrieved
1094 from <https://royalsocietypublishing.org/doi/10.1098/rsta.1970.0073>
1095 doi: 10.1098/rsta.1970.0073
- 1096 Hide, R., & Mason, P. (1975). Sloping convection in a rotating fluid. *Advances in*
1097 *Physics*, *24*(1), 47–100.
- 1098 Holmes, J. A., Lewis, S. R., & Patel, M. R. (2020). OpenMARS: A global record of
1099 martian weather from 1999 to 2015. *Plan. and Space Sci.*, *188*, 104962. doi: 10
1100 .1016/j.pss.2020.104962
- 1101 Hoskins, B. J., McIntyre, M., & Robertson, A. W. (1985). On the use and sig-
1102 nificance of isentropic potential vorticity maps. *Quarterly Journal of the Royal*
1103 *Meteorological Society*, *111*(470), 877–946.
- 1104 Irwin, P. G. J., Fletcher, L. N., Tice, D., Owen, S. J., Orton, G. S., Teanby, N. A.,
1105 & Davis, G. R. (2016). Time variability of Neptune’s horizontal and vertical
1106 cloud structure revealed by VLT/SINFONI and Gemini/NIFS from 2009 to
1107 2013. *Icarus*, *271*, 418-437. doi: 10.1016/j.icarus.2016.01.015
- 1108 Ivy, D. J., Solomon, S., Calvo, N., & Thompson, D. W. (2017). Observed connec-
1109 tions of arctic stratospheric ozone extremes to northern hemisphere surface
1110 climate. *Environmental Research Letters*, *12*(2), 024004.
- 1111 Jucker, M., Fueglistaler, S., & Vallis, G. K. (2014). Stratospheric sudden warmings
1112 in an idealized gcm. *Journal of Geophysical Research: Atmospheres*, *119*(19),
1113 11–054.
- 1114 Jukes, M. (1989). A shallow water model of the winter stratosphere. *J. Atmos. Sci.*,
1115 *46*, 2934-2956. doi: 10.1175/1520-0469(1989)046<2934:ASWMOT>2.0.CO;2
- 1116 Kang, W., & Tziperman, E. (2017). More frequent sudden stratospheric warming
1117 events due to enhanced mjo forcing expected in a warmer climate. *Journal of*

- 1118 *Climate*, 30(21), 8727–8743.
- 1119 Karkoschka, E. (2015). Uranus’ southern circulation revealed by Voyager 2: Unique
1120 characteristics. *Icarus*, 250, 294–307.
- 1121 Kaspi, Y., & Showman, A. P. (2015). Atmospheric dynamics of terrestrial exoplanets
1122 over a wide range of orbital and atmospheric parameters. *The Astrophysical
1123 Journal*, 804(1), 60.
- 1124 Kida, S. (1981). Motion of an elliptic vortex in a uniform shear flow. *Journal of the
1125 Physical Society of Japan*, 50(10), 3517–3520.
- 1126 Kidston, J., Scaife, A. A., Hardiman, S. C., Mitchell, D. M., Butchart, N., Baldwin,
1127 M. P., & Gray, L. J. (2015). Stratospheric influence on tropospheric jet
1128 streams, storm tracks and surface weather. *Nature Geoscience*, 8(6), 433.
- 1129 Kirchhoff, G. R. (1876). *Vorlesungen über mathematische physik: mechanik* (Vol. 1).
1130 Teubner.
- 1131 Kolstad, E. W., Breiteig, T., & Scaife, A. A. (2010). The association between
1132 stratospheric weak polar vortex events and cold air outbreaks in the northern
1133 hemisphere. *Quarterly Journal of the Royal Meteorological Society*, 136(649),
1134 886–893.
- 1135 Komacek, T. D., & Abbot, D. S. (2019). The atmospheric circulation and climate
1136 of terrestrial planets orbiting sun-like and m dwarf stars over a broad range of
1137 planetary parameters. *The Astrophysical Journal*, 871(2), 245.
- 1138 Krüger, K., Naujokat, B., & Labitzke, K. (2005). The unusual midwinter warming
1139 in the southern hemisphere stratosphere 2002: A comparison to northern
1140 hemisphere phenomena. *Journal of the atmospheric sciences*, 62(3), 603–613.
- 1141 Lait, L. (1994). An alternative form for potential vorticity. *J. Atmos. Sci.*, 51, 1754–
1142 1759.
- 1143 Lam, J. S.-L., & Dritschel, D. G. (2001). On the beta-drift of an initially circular
1144 vortex patch. *Journal of Fluid Mechanics*, 436, 107–129.
- 1145 Lebonnois, S., Burgalat, J., Rannou, P., & Charnay, B. (2012). Titan global climate
1146 model: a new 3-dimensional version of the IPSL Titan GCM. , 218, 707–722.
- 1147 Lee, C., Lewis, S. R., & Read, P. L. (2007). Superrotation in a Venus general circula-
1148 tion model. *Journal of Geophysical Research: Planets*, 112(E4).
- 1149 Lee, C., Lewis, S. R., & Read, P. L. (2010). A bulk cloud parameterization in a
1150 Venus general circulation model. *Icarus*, 206(2), 662–668.
- 1151 Li, C., Ingersoll, A. P., Klipfel, A. P., & Brettle, H. (2020). Modeling the stability of
1152 polygonal patterns of vortices at the poles of Jupiter as revealed by the Juno
1153 spacecraft. *Proceedings of the National Academy of Sciences*.
- 1154 Limaye, S. S., Kossin, J. P., Rozoff, C., Piccioni, G., Titov, D. V., & Markiewicz,
1155 W. J. (2009). Vortex circulation on Venus: Dynamical similarities with terres-
1156 trial hurricanes. *Geophysical Research Letters*, 36(4).
- 1157 Limaye, S. S., & Suomi, V. E. (1981). Cloud motions on venus: Global structure and
1158 organization. *Journal of the Atmospheric Sciences*, 38(6), 1220–1235.
- 1159 Lindgren, E., Sheshadri, A., & Plumb, R. (2018). Sudden stratospheric warming
1160 formation in an idealized general circulation model using three types of tro-
1161 pospheric forcing. *Journal of Geophysical Research: Atmospheres*, 123(18),
1162 10–125.
- 1163 Liu, Y., & Scott, R. (2015). The onset of the barotropic sudden warming in a global
1164 model. *Quarterly Journal of the Royal Meteorological Society*, 141(693), 2944–
1165 2955.
- 1166 Lora, J. M., Lunine, J. I., & Russell, J. L. (2015). Gcm simulations of Titan’s mid-
1167 dle and lower atmosphere and comparison to observations. *Icarus*, 250, 516–
1168 528.
- 1169 Lora, J. M., Tokano, T., d’Ollone, J. V., Lebonnois, S., & Lorenz, R. D. (2019).
1170 A model intercomparison of Titan’s climate and low-latitude environment.
1171 *Icarus*, 333, 113–126.

- 1172 Love, A. (1893). On the stability of certain vortex motions. *Proceedings of the Lon-*
 1173 *don Mathematical Society*, 1(1), 18–43.
- 1174 Luszcz-Cook, S., de Pater, I., Ádámkóvics, M., & Hammel, H. (2010). Seeing double
 1175 at Neptune’s south pole. *Icarus*, 208(2), 938–944.
- 1176 Luz, D., Berry, D., Piccioni, G., Drossart, P., Politi, R., Wilson, C., . . . Nuccilli, F.
 1177 (2011). Venus’s southern polar vortex reveals precessing circulation. *Science*,
 1178 332(6029), 577–580.
- 1179 Martineau, P., Chen, G., Son, S.-W., & Kim, J. (2018). Lower-stratospheric control
 1180 of the frequency of sudden stratospheric warming events. *Journal of Geophysi-*
 1181 *cal Research: Atmospheres*, 123(6), 3051–3070.
- 1182 Matthewman, N. J., & Esler, J. (2011). Stratospheric sudden warmings as self-
 1183 tuning resonances. part i: Vortex splitting events. *Journal of the atmospheric*
 1184 *sciences*, 68(11), 2481–2504.
- 1185 Mitchell, D., & Ball, E. (2021). Polar vortex review data.
 1186 doi: <https://doi.org/10.5523/bris.22xc4ls5z02y426k8raaezytkp>.
- 1187 Mitchell, D., Scott, R., Seviour, W., Thomson, S., Waugh, D., Teanby, N. A., &
 1188 Ball, E. (2021, June). *BrisClimate/polar_vortices_planetary_atmospheres:*
 1189 *Release of code for paper resubmission*. Zenodo. Retrieved from [https://](https://doi.org/10.5281/zenodo.5037244)
 1190 doi.org/10.5281/zenodo.5037244 doi: 10.5281/zenodo.5037244
- 1191 Mitchell, D. M., Gray, L. J., Anstey, J., Baldwin, M. P., & Charlton-Perez, A. J.
 1192 (2013). The influence of stratospheric vortex displacements and splits on
 1193 surface climate. *Journal of Climate*, 26(8), 2668–2682.
- 1194 Mitchell, D. M., Montabone, L., Thomson, S., & Read, P. L. (2015). Polar vortices
 1195 on Earth and Mars: A comparative study of the climatology and variability
 1196 from reanalyses. *Q. J. Roy. Meteor. Soc.*, 141, 550–562. doi: 10.1002/qj.2376
- 1197 Montabone, L., Marsh, K., Lewis, S. R., Read, P. L., Smith, M. D., Holmes, J.,
 1198 . . . Pamment, A. (2014). The Mars Analysis Correction Data Assimilation
 1199 (MACDA) dataset v1.0. *Geosci. Data J.*, 1, 129–139. doi: 10.1002/gdj3.13
- 1200 Montabone, L., Mitchell, D. M., Thomson, S. I., Read, P. L., & McConnochie, T. H.
 1201 (2014). The martian polar vortices in the ‘macda’ reanalysis: Climatology
 1202 and variability. In *5th international workshop on mars atmosphere: Mod-*
 1203 *elling and observations, oxford (uk)*. doi: [https://ui.adsabs.harvard.edu/abs/](https://ui.adsabs.harvard.edu/abs/2014mamo.conf.1307M/abstract)
 1204 [2014mamo.conf.1307M/abstract](https://ui.adsabs.harvard.edu/abs/2014mamo.conf.1307M/abstract)
- 1205 Montabone, L., Wordsworth, R., Aguiar, A., Jacoby, T., Manfrin, M., Read, P. L.,
 1206 . . . others (2010). Barotropic instability of planetary polar vortices: Civ anal-
 1207 ysis of specific multi-lobed structures. In *Hydralab iii joint transnational access*
 1208 *user meeting* (pp. 191–194). Retrieved from [https://hydralab.eu/uploads/](https://hydralab.eu/uploads/proceedings/CNRS-25_Montabone.pdf)
 1209 [proceedings/CNRS-25_Montabone.pdf](https://hydralab.eu/uploads/proceedings/CNRS-25_Montabone.pdf)
- 1210 Montabone, L., Wordsworth, R., Aguiar, A., Jacoby, T., Read, P. L., McCli-
 1211 mans, T., & Ellingsen, I. (2010). Barotropic instability of planetary pol-
 1212 ar vortices: Concept, experimental set-up and parameter space analysis.
 1213 *Proc. HYDRALAB III Joint User Meeting*, 194, 135–138. Retrieved from
 1214 https://hydralab.eu/uploads/proceedings/NTNU-16_Montabone.pdf
- 1215 Newman, C. E., Lee, C., Lian, Y., Richardson, M. I., & Toigo, A. D. (2011). Strato-
 1216 spheric superrotation in the TitanWRF model. *Icarus*, 213(2), 636–654.
- 1217 Nixon, C. A., Ansty, T. M., Lombardo, N. A., Bjoraker, G. L., Achterberg, R. K.,
 1218 Annex, A. M., . . . Flasar, F. M. (2019). Cassini Composite Infrared Spec-
 1219 trometer (CIRS) Observations of Titan 2004–2017. *Astrophysical Journal*
 1220 *Supplement Series*, 244(1), 14. doi: 10.3847/1538-4365/ab3799
- 1221 O’Neill, A., Oatley, C., Charlton-Perez, A. J., Mitchell, D., & Jung, T. (2017).
 1222 Vortex splitting on a planetary scale in the stratosphere by cyclogenesis on a
 1223 subplanetary scale in the troposphere. *Quarterly Journal of the Royal Meteor-*
 1224 *ological Society*, 143(703), 691–705.
- 1225 O’Neill, M. E., Emanuel, K. A., & Flierl, G. R. (2015). Polar vortex formation
 1226 in giant-planet atmospheres due to moist convection. *Nature Geoscience*, 8(7),

- 1227 523.
- 1228 O'Neill, M. E., Emanuel, K. A., & Flierl, G. R. (2016). Weak jets and strong cy-
- 1229 clones: Shallow-water modeling of giant planet polar caps. *Journal of the At-*
- 1230 *mospheric Sciences*, 73(4), 1841–1855.
- 1231 Orton, G., & Yanamandra-Fisher, P. (2005). Saturn's temperature field from high-
- 1232 resolution middle-infrared imaging. *Science*, 307(5710), 696–698.
- 1233 Orton, G. S., Encrenaz, T., Leyrat, C., Puetter, R., & Friedson, A. J. (2007). Ev-
- 1234 idence for methane escape and strong seasonal and dynamical perturbations
- 1235 of Neptune's atmospheric temperatures. *Astronomy & Astrophysics*, 473(1),
- 1236 L5–L8.
- 1237 Piccialli, A., Tellmann, S., Titov, D., Limaye, S., Khatuntsev, I., Pätzold, M., &
- 1238 Häusler, B. (2012). Dynamical properties of the Venus mesosphere from the
- 1239 radio-occultation experiment VeRa onboard Venus Express. *Icarus*, 217(2),
- 1240 669–681.
- 1241 Piccioni, G., Drossart, P., Sanchez-Lavega, A., Hueso, R., Taylor, F., Wilson, C., . . .
- 1242 others (2007). South-polar features on Venus similar to those near the north
- 1243 pole. *Nature*, 450(7170), 637.
- 1244 Polvani, L. M., & Dritschel, D. G. (1993). Wave and vortex dynamics on the surface
- 1245 of a sphere. *Journal of Fluid Mechanics*, 255, 35–64.
- 1246 Polvani, L. M., & Kushner, P. J. (2002). Tropospheric response to stratospheric
- 1247 perturbations in a relatively simple general circulation model. *Geophysical Re-*
- 1248 *search Letters*, 29(7), 18–1.
- 1249 Polvani, L. M., & Plumb, R. A. (1992). Rossby wave breaking, microbreaking,
- 1250 filamentation, and secondary vortex formation: The dynamics of a perturbed
- 1251 vortex. *Journal of the atmospheric sciences*, 49(6), 462–476.
- 1252 Polvani, L. M., Waugh, D., & Plumb, R. A. (1995). On the subtropical edge of
- 1253 the stratospheric surf zone. *Journal of the atmospheric sciences*, 52(9), 1288–
- 1254 1309.
- 1255 Rayleigh, J. W. S. (1880). On the stability or instability of certain fluid motions.
- 1256 *Proc. London Math. Soc.*, 11, 57–72.
- 1257 Read, P. (2011). Dynamics and circulation regimes of terrestrial planets. *Planetary*
- 1258 *and Space Science*, 59(10), 900–914.
- 1259 Read, P. L., & Lebonnois, S. (2018). Superrotation on Venus, on Titan, and else-
- 1260 where. *Annual Review of Earth and Planetary Sciences*, 46, 175–202.
- 1261 Read, P. L., Tabataba-Vakili, F., Wang, Y., Augier, P., Lindborg, E., Valeanu, A., &
- 1262 Young, R. M. (2018). Comparative terrestrial atmospheric circulation regimes
- 1263 in simplified global circulation models. part ii: Energy budgets and spectral
- 1264 transfers. *Quarterly Journal of the Royal Meteorological Society*, 144(717),
- 1265 2558–2576.
- 1266 Read, P. L., Yamazaki, Y., Lewis, S., Williams, P., Miki-Yamazaki, K., Somme-
- 1267 ria, J., . . . Fincham, A. (2004). Jupiter's and Saturn's convectively driven
- 1268 banded jets in the laboratory. *Geophysical Research Letters*, 31(22), L22701.
- 1269 Retrieved from <http://doi.wiley.com/10.1029/2004GL020106> doi:
- 1270 10.1029/2004GL020106
- 1271 Reinaud, J. N., & Dritschel, D. G. (2019). The stability and nonlinear evolution of
- 1272 quasi-geostrophic toroidal vortices. *J. Fluid Mech.*, 863, 60–78. doi: 10.1017/
- 1273 [jfm.2018.1013](https://doi.org/10.1017/jfm.2018.1013)
- 1274 Rong, P.-P., & Waugh, D. W. (2004). Vacillations in a shallow-water model
- 1275 of the stratosphere. *Journal of the Atmospheric Sciences*, 61(10), 1174 -
- 1276 1185. Retrieved from [https://journals.ametsoc.org/view/journals/](https://journals.ametsoc.org/view/journals/atasc/61/10/1520-0469_2004_061_1174_viasmo_2.0.co_2.xml)
- 1277 [atasc/61/10/1520-0469_2004_061_1174_viasmo_2.0.co_2.xml](https://journals.ametsoc.org/view/journals/atasc/61/10/1520-0469_2004_061_1174_viasmo_2.0.co_2.xml) doi:
- 1278 10.1175/1520-0469(2004)061<1174:VIASMO>2.0.CO;2
- 1279 Rostami, M., Zeitlin, V., & Montabone, L. (2018). On the role of spatially inho-
- 1280 mogeneous diabatic effects upon the evolution of Mars' annular polar vortex.
- 1281 *Icarus*, 314, 376–388.

- 1282 Rostami, M., Zeitlin, V., & Spiga, A. (2017). On the dynamical nature of Saturn's
1283 North Polar hexagon. *Icarus*, *297*, 59–70. Retrieved from [http://dx.doi](http://dx.doi.org/10.1016/j.icarus.2017.06.006)
1284 [.org/10.1016/j.icarus.2017.06.006](http://dx.doi.org/10.1016/j.icarus.2017.06.006) doi: 10.1016/j.icarus.2017.06.006
- 1285 Sánchez-Lavega, A., Lebonnois, S., Imamura, T., Read, P., & Luz, D. (2017). The
1286 atmospheric dynamics of Venus. *Space Science Reviews*, *212*(3), 1541–1616.
- 1287 Sanders, R. (2017). Keck observations reveal complex face of Uranus. *Berkeley News*
1288 *(Berkeley, CA) (2012)*.
- 1289 Sanz-Requena, J., Pérez-Hoyos, S., Sánchez-Lavega, A., Antuñaño, A., & Irwin,
1290 P. G. (2018). Haze and cloud structure of Saturn's north pole and hexagon
1291 wave from Cassini/ISS imaging. *Icarus*, *305*, 284–300.
- 1292 Sayanagi, K. M., Baines, K. H., Dyudina, U., Fletcher, L. N., Sánchez-Lavega, A., &
1293 West, R. A. (2018). Saturn's polar atmosphere. *Saturn in the 21st Century*,
1294 *20*, 337.
- 1295 Sayanagi, K. M., Blalock, J. J., Dyudina, U. A., Ewald, S. P., & Ingersoll, A. P.
1296 (2017). Cassini ISS observation of Saturn's north polar vortex and comparison
1297 to the south polar vortex. *Icarus*, *285*, 68–82.
- 1298 Schecter, D., Dubin, D., Fine, K., & Driscoll, C. (1999). Vortex crystals from 2d eu-
1299 ler flow: Experiment and simulation. *Physics of Fluids*, *11*(4), 905–914.
- 1300 Scherhag, R. (1952). Die explosionartigen stratosphärenwarmungen des spatwinters
1301 1951-1952. *Ber. Deut. Wetterd.*, *6*, 51–63.
- 1302 Schoeberl, M. R., & Hartmann, D. L. (1991). The dynamics of the stratospheric po-
1303 lar vortex and its relation to springtime ozone depletions. *Science*, *251*(4989),
1304 46–52.
- 1305 Scott, R. (2011). Polar accumulation of cyclonic vorticity. *Geophysical & Astrophys-
1306 ical Fluid Dynamics*, *105*(4-5), 409–420.
- 1307 Scott, R. K., & Polvani, L. M. (2006). Internal variability of the winter stratosphere.
1308 part i: Time-independent forcing. *J. Atmos. Sci.*, *63*(11), 2758–2776. doi: 10
1309 [.1175/JAS3797.1](https://doi.org/10.1175/JAS3797.1)
- 1310 Scott, R. K., Seviour, W. J. M., & Waugh, D. W. (2020). Forcing of the martian
1311 polar annulus by hadley cell transport and latent heating. *Q. J. R. Meteorol.*
1312 *Soc*, *146*, 2174–2190. doi: 10.1002/qj.3786
- 1313 Seviour, W. J. M., Gray, L. J., & Mitchell, D. M. (2016). Stratospheric polar vor-
1314 tex splits and displacements in the high-top cmip5 climate models. *Journal of*
1315 *Geophysical Research: Atmospheres*, *121*(4), 1400–1413.
- 1316 Seviour, W. J. M., Waugh, D. W., & Scott, R. K. (2017). The stability of Mars's an-
1317 nular polar vortex. *J. Atmos. Sci.*, *74*(5), 1533–1547. doi: 10.1175/JAS-D-16
1318 -0293.1
- 1319 Sharkey, J., Teanby, N. A., Sylvestre, M., Mitchell, D. M., Seviour, W. J., Nixon,
1320 C. A., & Irwin, P. G. (2020a). Mapping the zonal structure of Titan's north-
1321 ern polar vortex. *Icarus*, *337*, 113441.
- 1322 Sharkey, J., Teanby, N. A., Sylvestre, M., Mitchell, D. M., Seviour, W. J., Nixon,
1323 C. A., & Irwin, P. G. (2020b). Potential vorticity structure of Titan's polar
1324 vortices from Cassini CIRS observations. *Icarus*, 114030.
- 1325 Shell, K. M., & Held, I. M. (2004). Abrupt transition to strong superrotation in an
1326 axisymmetric model of the upper troposphere. *Journal of the atmospheric sci-*
1327 *ences*, *61*(23), 2928–2935.
- 1328 Sheshadri, A., Plumb, R. A., & Gerber, E. P. (2015). Seasonal variability of the
1329 polar stratospheric vortex in an idealized agcm with varying tropospheric wave
1330 forcing. *Journal of the Atmospheric Sciences*, *72*(6), 2248–2266.
- 1331 Showman, A. P., Cho, J. Y., & Menou, K. (2010). Atmospheric circulation of exo-
1332 planets. *Exoplanets*, *526*, 471–516.
- 1333 Spence, T. W., & Fultz, D. (1977, aug). Experiments on Wave-Transition Spec-
1334 tra and Vacillation in an Open Rotating Cylinder. *Journal of the Atmospheric*
1335 *Sciences*, *34*(8), 1261–1285. Retrieved from [http://journals.ametsoc.org/
1336 doi/10.1175/1520-0469\(1977\)034%3C1261:EOWTSA%3E2.0.CO;2](http://journals.ametsoc.org/doi/10.1175/1520-0469(1977)034%3C1261:EOWTSA%3E2.0.CO;2) doi:

- 10.1175/1520-0469(1977)034<1261:EOWTSA>2.0.CO;2
- 1337
1338 Sromovsky, L., de Pater, I., Fry, P., Hammel, H., & Marcus, P. (2015). High s/n
1339 Keck and Gemini AO imaging of Uranus during 2012–2014: new cloud pat-
1340 terns, increasing activity, and improved wind measurements. *Icarus*, *258*,
1341 192–223.
- 1342 Sromovsky, L., Hammel, H., de Pater, I., Fry, P., Rages, K., Showalter, M., . . . oth-
1343 ers (2012). Episodic bright and dark spots on Uranus. *Icarus*, *220*(1), 6–22.
- 1344 Sugimoto, N., Kouyama, T., & Takagi, M. (2019). Impact of data assimilation on
1345 thermal tides in the case of Venus Express wind observation. *Geophysical Re-*
1346 *search Letters*, *46*(9), 4573–4580.
- 1347 Suomi, V. (1974). The dynamical regime as revealed by the uv markings. In *Bulletin*
1348 *of the american astronomical society* (Vol. 6, p. 386).
- 1349 Suomi, V. E., & Limaye, S. S. (1978). Venus: Further evidence of vortex circulation.
1350 *Science*, *201*(4360), 1009–1011.
- 1351 Sylvestre, M., Teanby, N. A., Vatant d’Ollone, J., Vinatier, S., Bézard, B.,
1352 Lebonnois, S., & Irwin, P. G. J. (2020). Seasonal evolution of temper-
1353 atures in Titan’s lower stratosphere. *Icarus*, *344*, 113188. doi: 10.1016/
1354 j.icarus.2019.02.003
- 1355 Tan, X., & Showman, A. P. (2021). Atmospheric circulation of brown dwarfs and
1356 directly imaged exoplanets driven by cloud radiative feedback: global and
1357 equatorial dynamics. *Monthly Notices of the Royal Astronomical Society*.
- 1358 Taylor, Diner, D., Elson, L., Hanner, M., McCleese, D., Martonchik, J., . . . others
1359 (1979). Infrared remote sounding of the middle atmosphere of Venus from the
1360 Pioneer orbiter. *Science*, *203*(4382), 779–781.
- 1361 Taylor, F. W. (2010). Planetary atmospheres. *Meteorological Applications*, *17*(4),
1362 393–403.
- 1363 Taylor, F. W. (2014). *The scientific exploration of venus*. Cambridge University
1364 Press.
- 1365 Teanby, N., de Kok, R., Irwin, P., Osprey, S., Vinatier, S., Gierasch, P., . . . others
1366 (2008). Titan’s winter polar vortex structure revealed by chemical tracers.
1367 *Journal of Geophysical Research: Planets*, *113*(E12).
- 1368 Teanby, N. A., Bézard, B., Vinatier, S., Sylvestre, M., Nixon, C. A., Irwin, P. G.,
1369 . . . Flasar, F. M. (2017). The formation and evolution of Titan’s winter polar
1370 vortex. *Nature communications*, *8*(1), 1586.
- 1371 Teanby, N. A., Irwin, P. G. J., de Kok, R., & Nixon, C. A. (2009). Dynamical
1372 implications of seasonal and spatial variations in Titan’s stratospheric compo-
1373 sition. *Philosophical Transactions of the Royal Society of London Series A*,
1374 *367*(1889), 697–711. doi: 10.1098/rsta.2008.0164
- 1375 Teanby, N. A., Irwin, P. G. J., Nixon, C. A., de Kok, R., Vinatier, S., Couste-
1376 nis, A., . . . Flasar, F. M. (2012). Active upper-atmosphere chemistry and
1377 dynamics from polar circulation reversal on Titan. , *491*, 732–735. doi:
1378 10.1038/nature11611
- 1379 Teanby, N. A., Sylvestre, M., Sharkey, J., Nixon, C. A., Vinatier, S., & Ir-
1380 win, P. G. J. (2019). Seasonal evolution of Titan’s stratosphere dur-
1381 ing the Cassini mission. *Geophys. Res. Letters*, *46*(6), 3079–3089. doi:
1382 10.1029/2018GL081401
- 1383 Thompson, D. W., Solomon, S., Kushner, P. J., England, M. H., Grise, K. M., &
1384 Karoly, D. J. (2011). Signatures of the antarctic ozone hole in southern hemi-
1385 sphere surface climate change. *Nature Geoscience*, *4*(11), 741–749.
- 1386 Thomson, J. J. (1883). *A treatise on the motion of vortex rings: an essay to which*
1387 *the adams prize was adjudged in 1882, in the university of cambridge*. Macmil-
1388 lan.
- 1389 Thomson, S. I., & McIntyre, M. E. (2016). Jupiter’s unearthly jets: A new turbulent
1390 model exhibiting statistical steadiness without large-scale dissipation. *Journal*
1391 *of the Atmospheric Sciences*, *73*(3), 1119–1141.

- 1392 Thomson, S. I., & Vallis, G. K. (2019a, jul). The effects of gravity on the climate
1393 and circulation of a terrestrial planet. *Quarterly Journal of the Royal Meteorological Society*, *145*(723), 2627–2640. Retrieved from [https://onlinelibrary](https://onlinelibrary.wiley.com/doi/abs/10.1002/qj.3582)
1394 [.wiley.com/doi/abs/10.1002/qj.3582](https://onlinelibrary.wiley.com/doi/abs/10.1002/qj.3582) doi: 10.1002/qj.3582
1395
- 1396 Thomson, S. I., & Vallis, G. K. (2019b). Hierarchical modeling of solar system plan-
1397 ets with isca. *Atmosphere*, *10*(12), 803.
- 1398 Toigo, A. D., Waugh, D. W., & Guzewich, S. D. (2017, January). What causes
1399 Mars’ annular polar vortices? , *44*(1), 71-78. doi: 10.1002/2016GL071857
- 1400 Tollefson, J., de Pater, I., Marcus, P. S., Luszcz-Cook, S., Sromovsky, L. A., Fry,
1401 P. M., ... Wong, M. H. (2018). Vertical wind shear in Neptune’s upper at-
1402 mosphere explained with a modified thermal wind equation. *Icarus*, *311*,
1403 317–339.
- 1404 Vinatier, S., Mathé, C., Bézard, B., Vatant d’Ollone, J., Lebonnois, S., Dauphin,
1405 C., ... Jennings, D. E. (2020). Temperature and chemical species dis-
1406 tributions in the middle atmosphere observed during Titan’s late northern
1407 spring to early summer. *Astronomy and Astrophysics*, *641*, A116. doi:
1408 10.1051/0004-6361/202038411
- 1409 Vinatier, S., Schmitt, B., Bézard, B., Rannou, P., Dauphin, C., de Kok, R., ...
1410 Flasar, F. M. (2018). Study of Titan’s fall southern stratospheric polar cloud
1411 composition with Cassini/CIRS: Detection of benzene ice. *Icarus*, *310*, 89–104.
1412 doi: 10.1016/j.icarus.2017.12.040
- 1413 Wang, H. (2007). Dust storms originating in the northern hemisphere during the
1414 third mapping year of Mars Global Surveyor. *Icarus*, *189*(2), 325–343.
- 1415 Wang, H., & Richardson, M. I. (2015, May). The origin, evolution, and trajec-
1416 tory of large dust storms on Mars during Mars years 24-30 (1999-2011). , *251*,
1417 112-127. doi: 10.1016/j.icarus.2013.10.033
- 1418 Wang, Y., Read, P. L., Tabataba-Vakili, F., & Young, R. M. (2018). Compara-
1419 tive terrestrial atmospheric circulation regimes in simplified global circulation
1420 models. part i: From cyclostrophic super-rotation to geostrophic turbulence.
1421 *Quarterly Journal of the Royal Meteorological Society*, *144*(717), 2537–2557.
- 1422 Waugh, D. W., & Dritschel, D. G. (1991). The stability of filamentary vorticity
1423 in two-dimensional geophysical vortex-dynamics models. *J. Fluid Mech.*, *231*,
1424 575-598. doi: 10.1017/S002211209100352X
- 1425 Waugh, D. W., & Polvani, L. M. (2010). Stratospheric polar vortices.
- 1426 Waugh, D. W., Sobel, A. H., & Polvani, L. M. (2017). What is the polar vortex and
1427 how does it influence weather? *Bulletin of the American Meteorological Soci-*
1428 *ety*, *98*(1), 37–44.
- 1429 Waugh, D. W., Toigo, A. D., Guzewich, S. D., Greybush, S. J., Wilson, R. J., &
1430 Montabone, L. (2016). Martian polar vortices: Comparison of reanalyses. *J.*
1431 *Geophys. Res. Planets*, *121*. doi: 10.1002/2016JE005093
- 1432 Wood, R. B., & McIntyre, M. E. (2010). A general theorem on angular-momentum
1433 changes due to potential vorticity mixing and on potential-energy changes due
1434 to buoyancy mixing. *Journal of the atmospheric sciences*, *67*(4), 1261–1274.
- 1435 Wright, C., Banyard, T., Hall, R., Hindley, N., Mitchel, D., & Seviour, W. (2021).
1436 The january 2021 sudden stratosphericwarming in aeolus and mls observations.
1437 *Weather and Climate Dynamics, in prep.*
- 1438 Yamamoto, M., & Takahashi, M. (2006). Superrotation maintained by meridional
1439 circulation and waves in a Venus-like AGCM. *Journal of the atmospheric sci-*
1440 *ences*, *63*(12), 3296–3314.
- 1441 Yamamoto, M., & Takahashi, M. (2015). Dynamics of polar vortices at cloud top
1442 and base on Venus inferred from a general circulation model: case of a strong
1443 diurnal thermal tide. *Planetary and Space Science*, *113*, 109–119.

1444 **Acknowledgments**

1445 D.M is funded under a NERC research fellowship (NE/N014057/1). N.A.T is funded by
1446 the UK Science and Technology Facilities Council and the UK Space Agency (ST/M007715/1,
1447 ST/R000980/1, ST/R001367/1). E.B is funded by a NERC GW4+ Doctoral Training
1448 Partnership studentship from the Natural Environmental Research Council (NE/S007504/1).
1449 The authors would like to thank Norihiko Sugimoto for providing the data used to cre-
1450 ate Figure 1a, Cheng Li and Alexandra Klipfel for providing the data for Figure 8, and
1451 Michael McIntyre and Mark Hammond for useful discussions. We thank Luca Montabone
1452 and the two anonymous reviewers for their insightful and thorough reviews.

1453 **Data Availability Statement**

1454 The atmospheric model and observation data used for the original figures in the
1455 study (Figure 1, 6 and 9) are available at the University of Bristol data repository, data.bris,
1456 via <https://doi.org/10.5523/bris.22xc4ls5z02y426k8raaezytkp> (D. Mitchell & Ball, 2021).
1457 For all other figures the source citation or repository is given in the caption of the fig-
1458 ure. All plotting code is available in D. Mitchell et al. (2021).

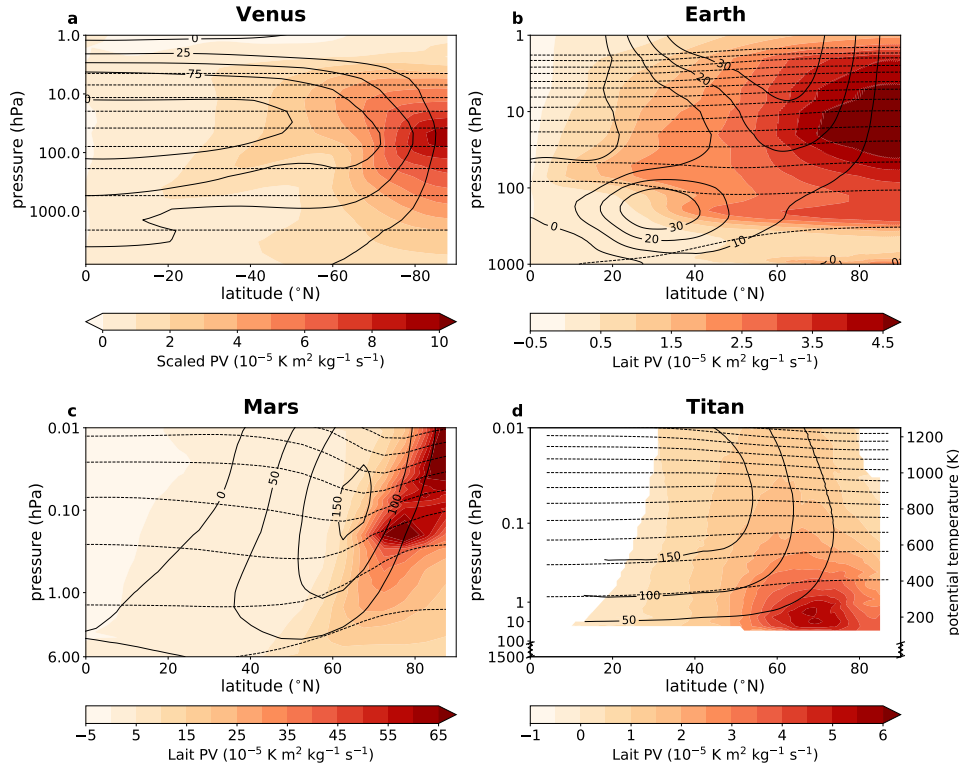


Figure 1. Winter zonal PV and zonal wind cross-sections as a function of altitude for Venus (a), Earth (b), Mars (c) and Titan (d). a) Southern hemisphere monthly-mean zonal-mean scaled potential vorticity (shading, scaling and PV calculations according to Piccialli et al. (2012); Garate-Lopez et al. (2016)), zonal wind (solid contours, units of ms^{-1}), and potential temperature (dashed contours, corresponding to 300, 400, ... K). b-d) Northern hemisphere monthly-mean zonal-mean Lait-scaled potential vorticity (shading, (Lait, 1994)), zonal wind (solid contours, units of ms^{-1}), and potential temperature (dashed contours, corresponding to 200, 300 ... K). Data are taken from the following sources: a) 30 Earth days (28th March - 26th April 2008) of the AFES-Venus GCM with VALEDAS data assimilation, described in Sugimoto et al. (2019); b) the ERA5 reanalysis dataset, averaged over December-January-February for 1979-2019; c) the OpenMARS reanalysis dataset, averaged over Ls 255-285° from MY 24-32; d) analysis of Cassini CIRS data from Sharkey et al. (2020b), averaged over Ls 325-345° (September 2006 - April 2008). The compressed axis represents Titan’s troposphere. Note that positive winds are defined as in the direction of the rotation of the planet, which for Venus is in the opposite sense to the other planets. Figure adapted from (Vaugh et al., 2016; Ball et al., 2021; Sharkey et al., 2020b; D. Mitchell & Ball, 2021)

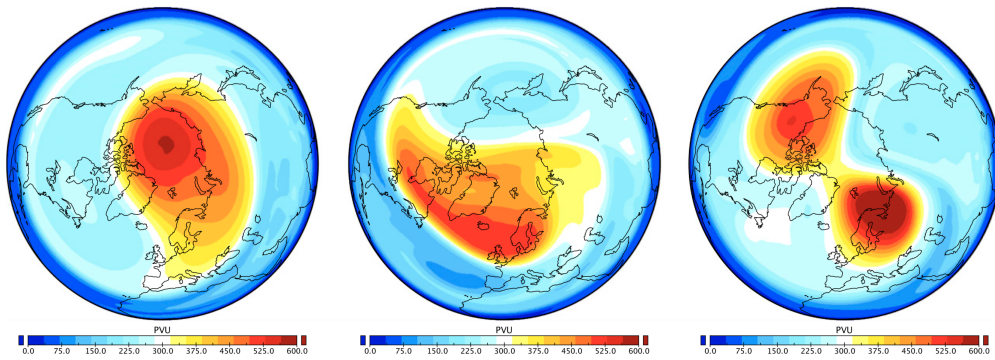


Figure 2. The different states of Earth's northern hemisphere stratospheric polar vortex. Northern polar stereographic plots of snapshots of Ertel (theta-normalised) potential vorticity in the mid stratosphere (10 hPa, ~30 km) during (left) a stable period, (middle) a vortex displaced period, and (right) vortex split period. Units are Potential Vorticity Units (PVU). (Kang & Tziperman, 2017)

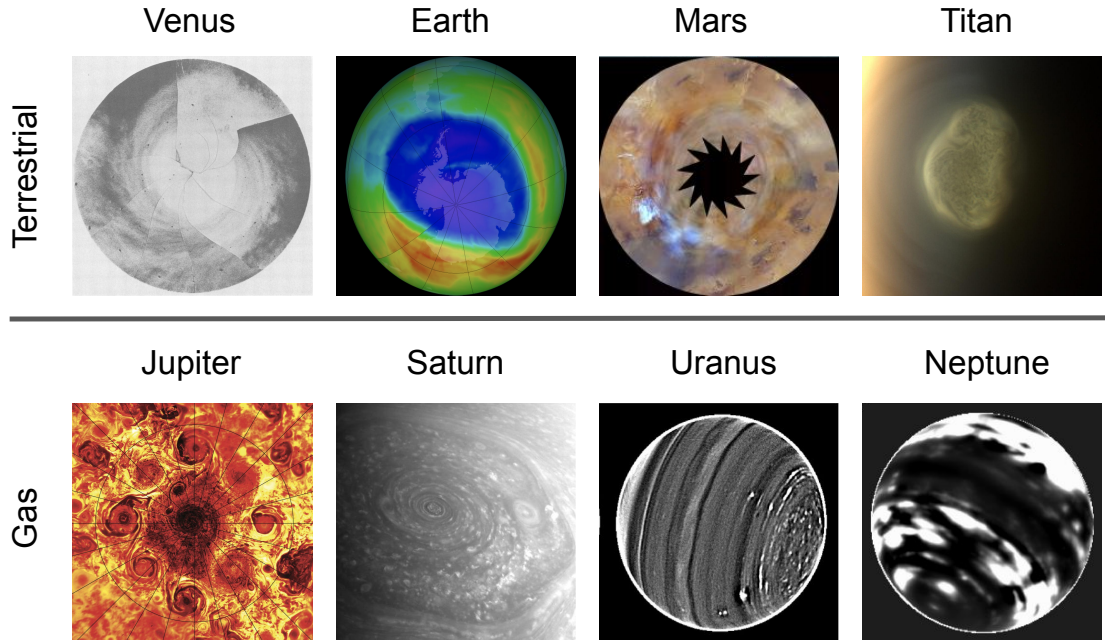


Figure 3. Example images which capture the varied nature of polar vortices on different planets and moons. The Venus panel shows a time-composite of images in the UV of the south polar region. The first image was taken on day 38 of 1974, and each segment of the composite shows an image taken ~ 12 hours after this first (V. E. Suomi & Limaye, 1978). Earth image shows the south polar region, and is total column ozone for Sept 13, 2014 from the Ozone Monitoring Instrument (OMI) instrument on the NASA Aura satellite (<https://visibleearth.nasa.gov/images/84382/un-panel-ozone-layer-on-the-road-to-recovery/84382f>). The ozone is calculated from solar back-scatter radiation in the visible and ultraviolet. Mars image is of the northern polar region ($40\text{-}90^\circ\text{N}$) taken on October the 22nd, 2012, from a MARCI/MRO colour composite, which highlights dust activity (NASA / JPL / MSSS). Titan image shows the south polar region, taken in false colour by ISS/Cassini (image from NASA/JPL-Caltech/Space Science Institute). Jupiter image shows the northern Type II polar vortex, taken in IR from the Juno spacecraft on the 2nd of February 2017. A latitude circle is shown at 80N (Adriani et al., 2018). The Saturn image shows the north polar region taken in the visible with ISS/Cassini (NASA/JPL-Caltech/Space Science Institute). Uranus image shows the north polar region ($\sim 100^\circ$ clockwise of the centre) as an enhanced adaptive optics near-IR image from the Keck II telescope, taken on 26th of July, 2012 (Sromovsky et al., 2015). Neptune image is an enhanced near-IR H-band adaptive optics image from the Keck II telescope, taken on July 3rd, 2013 (Tollefson et al., 2018).

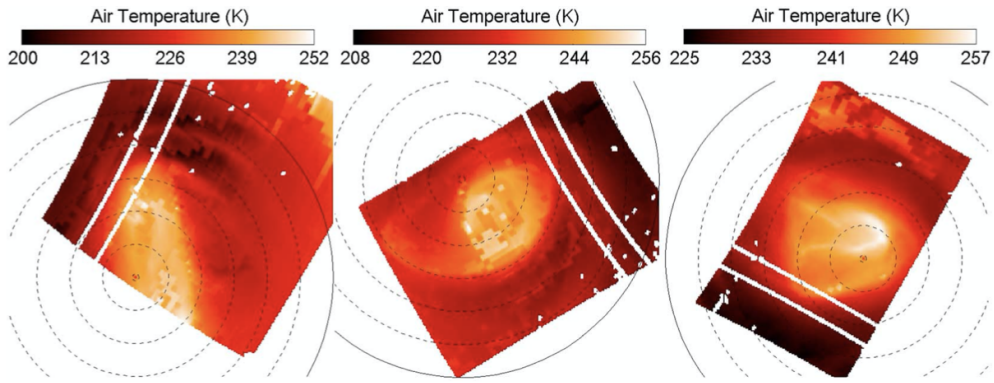


Figure 4. The air-temperature of the 330K isentropic surface of the southern hemisphere on Venus showing the vortex core (brighter regions) and wider vortex structure (darker regions). This is around the upper cloud level (~ 58 km). The panels show data derived from three different orbits of the Venus Express, which are orbits (left) 038, (middle) 310, and (right) 475. The estimated error is about 9 K on average. Latitude circles are plotted at 5° intervals from the south pole. The white pixels and lines are due to the lack of thermal information. Figure from Garate-Lopez et al. (2016).

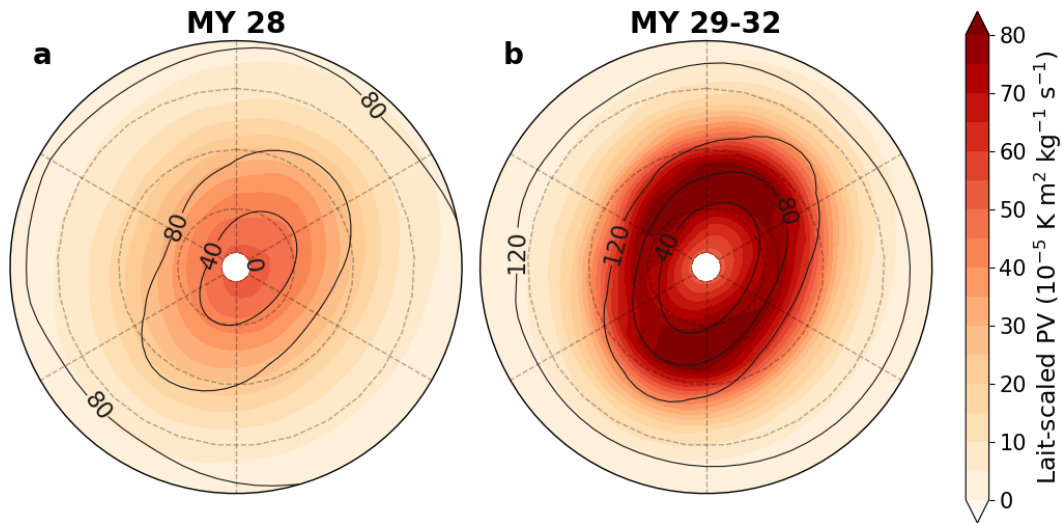


Figure 5. Mars' northern hemisphere polar vortex during a dust storm. Northern polar stereographic winter averages of Lait-scaled potential vorticity (shading) and zonal winds (contours) on the 350K potential temperature surface. (a) The polar vortex during the Martian Year (MY) 28 global dust storm, and (b) the polar vortex averaged over MY 29-32, during which time there were no global dust storms. Data are extracted from the OpenMARS reanalysis dataset and averaged over $L_s = 255 - 285^\circ$. Panels are bounded at 50°N and dashed lines of latitude are at intervals of 10°N . Figure adapted from (Ball et al., 2021).

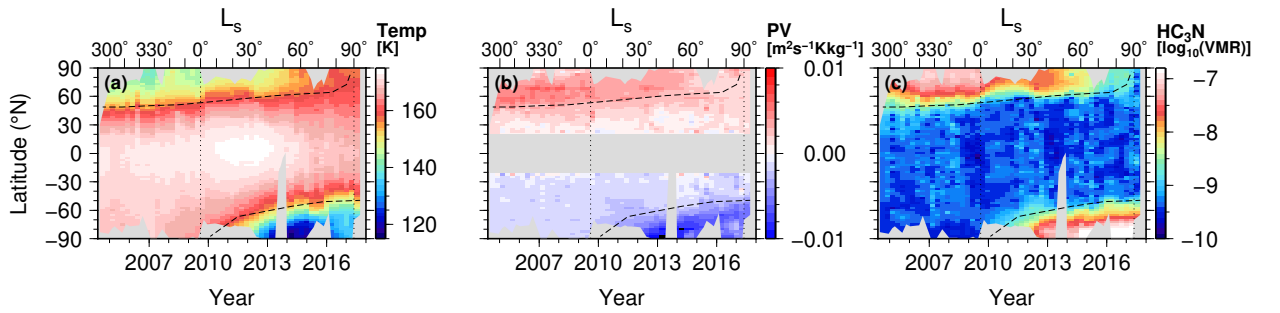


Figure 6. Titan’s polar vortex structure and evolution observed by Cassini CIRS. (a) Temperature at 1 hPa (Sharkey et al., 2020b) showing cold mid-stratosphere temperatures within the polar vortices. (b) PV at 0.1 hPa (Sharkey et al., 2020b) showing strong PV gradients near the vortex edge and an annular PV structure, with peak PV at $\sim 65^\circ$. (c) HC_3N volume mixing ratio (VMR) (Teanby et al., 2019) showing confinement of a short lifetime (\ll a Titan year) gas within the polar vortex. Dotted vertical lines are the 2009 northern spring equinox and 2017 northern summer solstice. Dashed regions indicate approximate edge of northern and southern vortices.

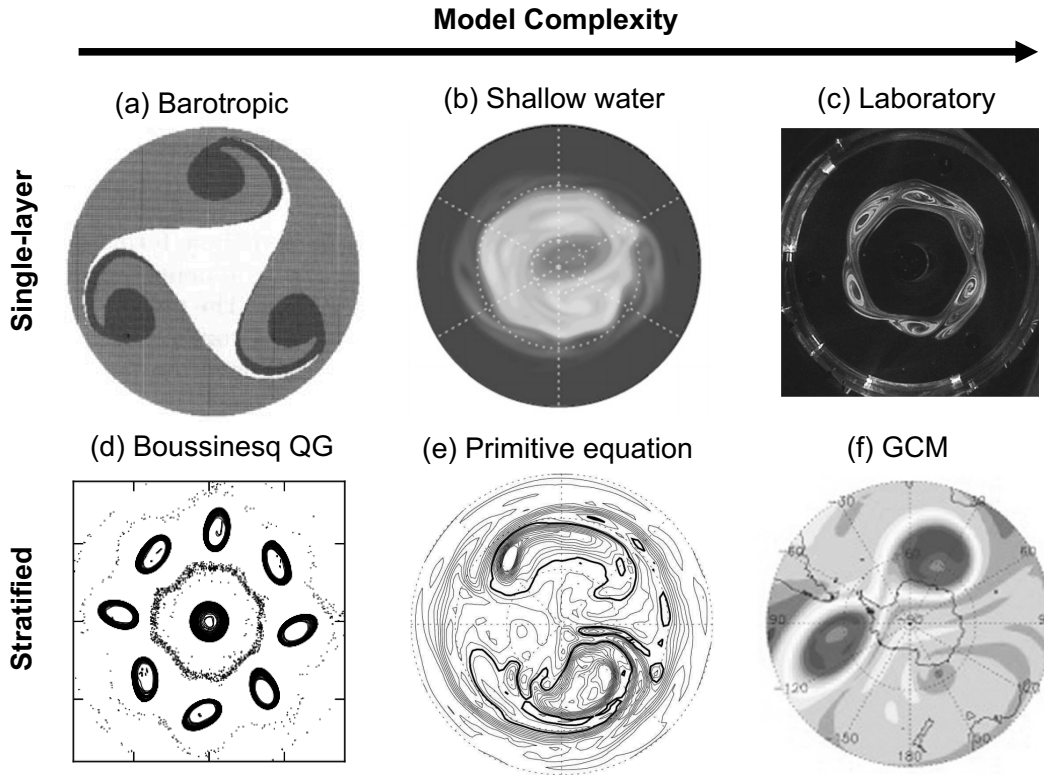


Figure 7. Major features of planetary polar vortices as simulated in a hierarchy of single-layer and stratified models of varying complexity. a) Instability of a Mars- or Titan-like annular vortex in a nondivergent barotropic model (Dritschel & Polvani, 1992). b) Mars-like annular polar vortex simulated in a divergent barotropic (shallow water) model with thermal relaxation (Seiour et al., 2017). c) Saturn-like hexagonal jet in a rotating tank laboratory experiment (Aguar et al., 2010). d) Jupiter-like multiple-vortex equilibrium in a quasi-geostrophic Boussinesq simulation (Reinaud & Dritschel, 2019). e) Earth-like stratospheric polar vortex splitting event simulated in a dry primitive equation model with Newtonian relaxation of temperature (Scott & Polvani, 2006). f) Forecast of the 2002 Antarctic sudden stratospheric warming in a comprehensive GCM (A. O’Neill et al., 2017).

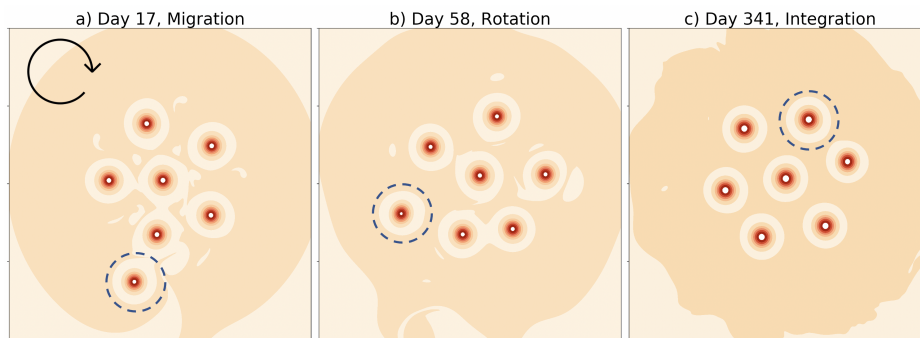


Figure 8. A simulation of Jupiter’s vortex clusters, showing a) an intruder migrating in, b) rotation of that intruder around the main cluster, and c) integration of the intruder into the main cluster. The vortex of interest has a dashed circle around it. The direction of rotation of the configuration is given in the left panel. Figure adapted from Li et al. (2020).

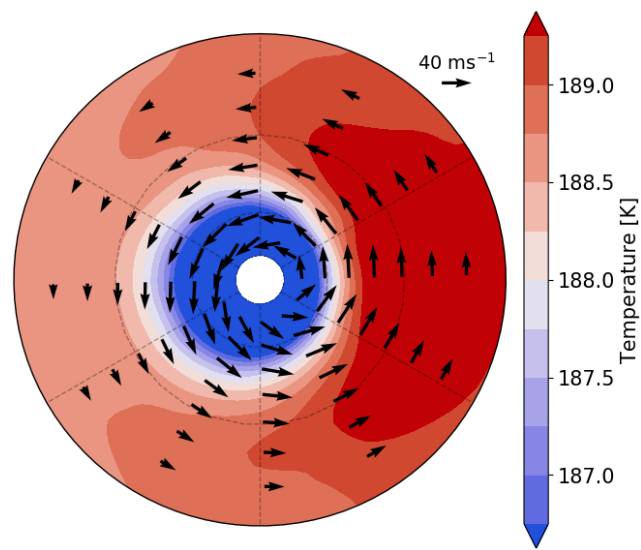


Figure 9. Northern polar stereographic plot of temperature (shading) and zonal wind (vectors) on the 5 hPa level from model simulations of TRAPPIST-1e. Dashed lines correspond to 30,60°N and the figure is bounded at the equator. Data is taken from the HAb1 Unified Model experiment from Fauchez et al. (2020).